

Document downloaded from:

<http://hdl.handle.net/10251/192715>

This paper must be cited as:

Maiti, B.; Abramov, A.; Pérez-Ruiz, R.; Díaz Díaz, D. (2019). The prospect of Photochemical Reactions in Confined Gel Media. *Accounts of Chemical Research*. 52(7):1865-1876.
<https://doi.org/10.1021/acs.accounts.9b00097>



The final publication is available at

<https://doi.org/10.1021/acs.accounts.9b00097>

Copyright American Chemical Society

Additional Information

The Prospect of Photochemical Reactions in Confined Gel Media

Binoy Maiti,^a Alex Abramov,^a Raúl Pérez-Ruiz,^b David Díaz Díaz^{*a,c}

^aInstitut für Organische Chemie, Universität Regensburg, Universitätsstr. 31, 93053 Regensburg, Germany

^bDepartamento de Química, Universitat Politècnica de València, Camino de Vera s/n, 46022, Valencia, Spain

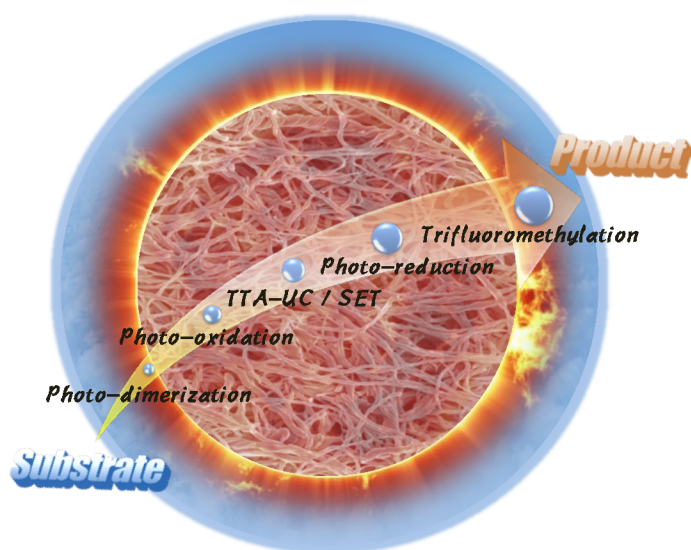
^cInstituto de Productos Naturales y Agrobiología del CSIC, Avda. Astrofísico Francisco Sánchez 3, 38206 La Laguna, Tenerife, Spain

*E-mail: David.Diaz@chemie.uni-regensburg.de; d.diaz.diaz@csic.es

CONSPECTUS

Nature is capable *per se* to control kinetics, conversion and selectivity of biochemical processes by means of confined reaction environments such as enzyme pockets, bilayer membranes, micelles, vesicles, cells or bioorganic frameworks. The main reason for this fact is the optimal molecular alignment and restricted motion of reactant molecules compared to those found in bulk solution. Under this inspiration, a number of synthetic photonanoreactors based on supramolecular self-assembled systems have been developed during the last decades, including mesoporous inorganic materials, microemulsions, micelles, vesicles, lipid bilayers foams, polyelectrolyte nanoparticles, etc. In a broader sense, nanoreactors technology constitutes nowadays a promising tool to enhance organic synthesis under sustainable reaction conditions. In general, nanoreactors change the essential properties of the molecules within them, thus affecting their chemical reactivity. Among the nanoreactor-like systems described in the literature to facilitate photochemical processes, the more recent use of viscoelastic supramolecular gels, typically made of low-molecular-weight (LMW) compounds self-assembled through non-covalent interactions, as compartmentalized reaction media is particularly appealing due to the versatility of these materials in terms of fabrication, properties and processability. Furthermore, the high specific surface areas found in supramolecular gels, their stimuli-responsive reversibility, good diffusion properties -enhancing the interactions between reactants and the

three dimensional (3D) porous network-, functional tuneability and blocking effect of external oxygen, are some of the most important features that can benefit photoinduced processes carried out in confined gel media. Not surprisingly, the efficiency of photochemical processes inside gel media is largely dependent on the type of reaction, characteristics of the gel network, solvent nature, reactants properties and reaction conditions. Thus, the main focus of this report is to provide a concise overview of the most relevant examples reported by us and others in order to illustrate the main advantages associated to the emerging use of gel-based materials as non-conventional reaction media to facilitate and control photochemical reactions. In particular, photodimerization, triplet-triplet annihilation upconversion (TTA-UC) coupled to single electron transfer (SET), photooxidation, photoreduction and trifluoromethylation reactions will be illustrated during the discussion. These examples suggest that gel-based media can provide a versatile platform for the discovery of new reaction pathways and facilitate the way that photochemical reactions are traditionally carried out in academia and industry in terms of reaction conditions and required infrastructure. In addition, the use of physical or chemical gels as reaction systems may also accelerate high-throughput screening of photocatalysts. Overall, a judicious choice of gelators, reactants, solvent and reaction conditions for the assembly of these gelators is crucial for controlling conversion, kinetics and selectivity of intragel photo-induced processes.



INTRODUCTION

Over millions of years of evolution, nature has optimized confined and compartmentalized environments such as cell organelles to carry out sophisticated chemical reactions with a precise control of kinetics and selectivity. This has inspired research groups all over the world to develop artificial nanoreactors based on hierarchical self-assembly of low-molecular-weight (LMW) molecules through non-covalent interactions (e.g. hydrogen-bonding, van der Waals, charge-transfer, dipolar, π - π stacking).^{1,2} In this context, photochemistry is a major beneficiary of reactivity in confined spaces, including for example mesoporous inorganic materials,³ microemulsions,⁴ micelles,^{5,6,7} vesicles,⁸ lipid bilayers⁹ foams,¹⁰ polyelectrolyte nanoparticles¹¹ and gels.^{12,13} In general, the proper confinement of reactants in these media improve photochemical processes by enhancing key properties such as light absorption and the lifetime of redox intermediates.^{14,15}

Among the above-mentioned non-conventional reaction media, supramolecular gels¹⁶ are typically made of LMW compounds (i.e. gelators) self-assembled through non-covalent interactions. The solid-like appearance and mechanical properties of these materials result from the immobilization of the liquid (major component) into the interstices of a self-assembled solid matrix (minor component) due to surface tension and capillary forces. The generation of the 3D-network linked thorough numerous junction points derives from an effective entanglement of 1D-strands of gelator molecules, usually of nm diameters and mm lengths, which can increase the viscosity of the medium by factors up to 10^{10} . In contrast to most covalently crosslinked polymer gels, supramolecular gels usually display reversible *gel-to-sol* phase transitions, which can be triggered by a variety of external stimuli responses (e.g. irradiation, temperature, pH, ionic strength). This feature constitutes an important asset for the recycling of the gel media. At this point, it is important to realize that aerobic environments do not compromise the high efficiency of biochemical processes that occur in nature involving different reactive intermediates. In this sense, molecular compartmentalization overcome potential deactivation pathways while enhancing the desired chemical route. Thus, supramolecular gels displaying high specific surface areas, stimuli-responsive reversibility, good diffusion properties and functional tuneability, have recently been identified with a remarkable prospective to mimic compartmentalization of complex natural systems to perform photochemical reactions that are

1
2
3 otherwise more difficult to do. Furthermore, the viscoelastic nature of gel-based materials may
4 also help to reduce overconcentration and overheating effects compared to more rigid systems.
5

6 Herein, we wish to provide a brief insight into the potential advantages of carrying out
7 photochemical processes in gels as confining and non-conventional reaction media.
8 Photopolymerization/photo-induced gelation processes¹⁷ and other catalytic reactions (i.e.
9 without using light irradiation) inside gel media are out of the scope of this contribution.¹⁸
10
11
12
13
14

15 **PHOTODIMERIZATION**

16
17 Motivated by the desire of gaining control on product selectivity, the well-established
18 photodimerization of acenaphthylene (ACN) has been studied in different nanoreactor systems
19 such as nanocapsule, micellar media, polymeric systems, zeolites, clay environments or liquid
20 crystalline systems.^{19,20} Maitra *et al.* showed for the first time that ACN photodimerization
21 (Figure 1) in supramolecular hydrogels made of LMW bile acids as reaction media took place
22 with higher selectivity than in homogeneous solution.²¹ Specifically, this group reported
23 photodimer ratios *syn:anti* (**2:3**) 3-10 times higher than the ratio in aqueous or micellar solutions
24 [e.g. sodium dodecyl sulfate (SDS), cetyltrimethylammonium bromide (CTAB), etc.].
25 Furthermore, when this reaction was further investigated by using different gelators (Figure 1,
26 gelators **4-7**), the *syn/anti* dimer ratios were found to be largely dependent on the hydrogel
27 rheological properties. Thus, the gels with highest rigidity also showed the highest product
28 selectivity, following the order **6 > 5 > 7 > 4**.
29
30
31
32
33
34
35
36
37
38
39
40
41
42
43
44
45
46
47
48
49
50
51
52
53
54
55
56
57
58
59
60

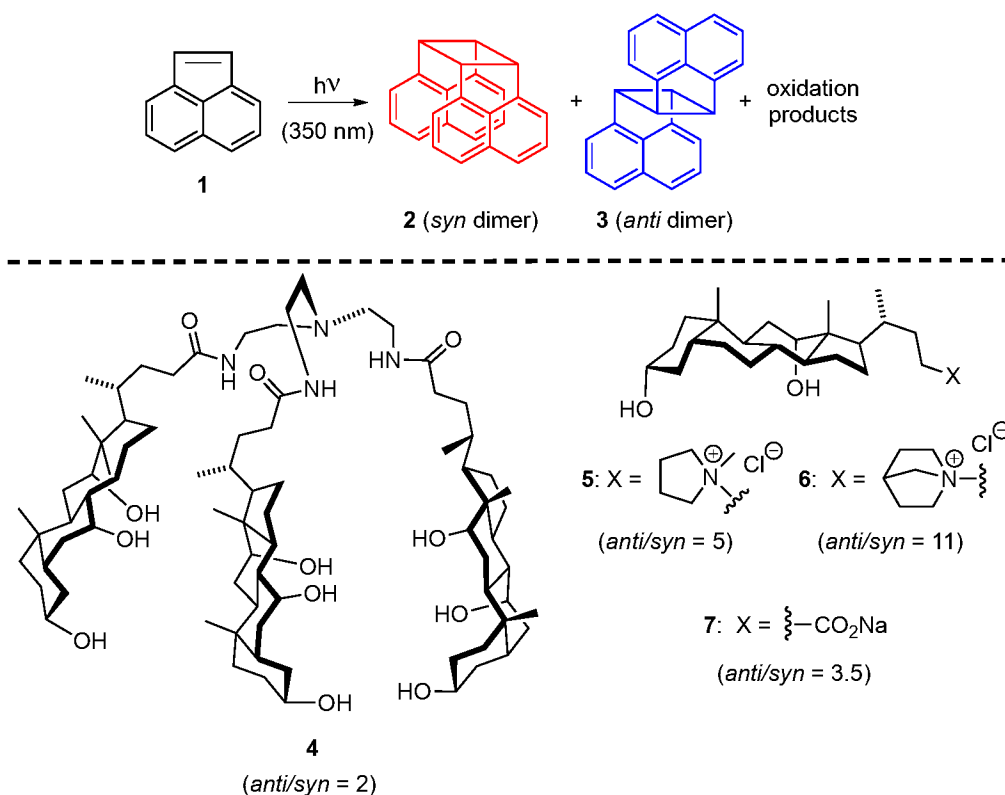


Figure 1. Photodimerization reaction of acenaphthylene (**1**) (*top*) carried out in supramolecular hydrogels made of different LMW gelators **4-7** (*bottom*). *Anti/syn* dimer ratios obtained with each gelator are given in brackets.

In 2009, Shinkai *et al.* studied the photodimerization of anthracene carboxylic acid inside a binary gelator based on 3,4,5-tris(*n*-dodecyloxy)benzoylamide substituted D-alanine (Figure 2).²² Interestingly, the results revealed that only two products (*anti*- and *syn*- head-to-head) were obtained in the gel matrix, differing from the production of the four different [4 + 4] cyclodimers in cyclohexane solution. These early studies put in the spotlight the potential of gel networks to drastically influence the selectivity of photo-induced processes.

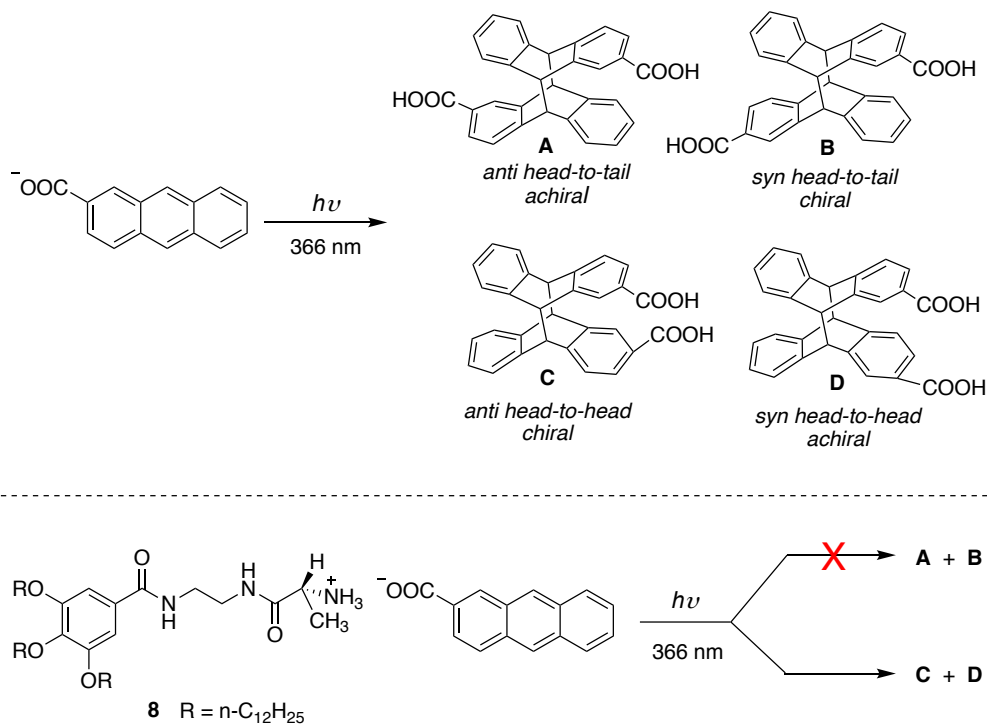


Figure 2. Schematic representation of [4 + 4] photocyclodimerization of 2-anthracenecarboxylic acid in the free state (*top*) and in the cyclohexane gel of binary system **8** (*bottom*) showing the products obtained in each case.

TRIPLET FUSION UPCONVERSION

Photon upconversion (UC) based on triplet-triplet annihilation (TTA) has attracted considerable interest during the last decade due to its low excitation power density demand (ambient sunlight) and readily tunable excitation/emission wavelengths. Indeed, it is also a safer, practically and economically more viable option than commercial UV sources. This technology, which has been successfully applied in different areas such as photocatalysis, photovoltaics, artificial photosynthesis, optics, etc., is capable of transforming visible into UV light involving a bimolecular system (i.e. a sensitizer or donor and an emitter or acceptor) and the connection of multistep photochemical pathways (Figure 3). Briefly, after the absorption of low-energy photons ($h\nu_1$), the triplet excited state (T_1) of the donor (sensitizer) is produced by intersystem crossing (ISC) from the singlet excited state (S_1). Subsequently, triplets of the acceptor (emitter) are populated by triplet-triplet energy transfer (TTET) from the triplets of the sensitizer (Dexter mechanism). When two acceptor molecules in their triplet states are capable of colliding during

their lifetimes, a higher singlet energy level is formed by TTA and, consequently, generates delayed upconverted fluorescence ($h\nu_2$).²³

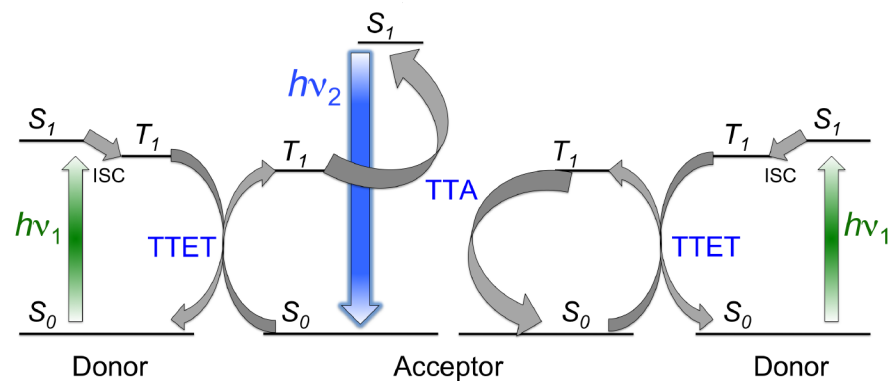


Figure 3. Simplified Jablonski diagram illustrating the mechanism of TTA-UC showing the main energy levels involved in the process (S = singlet, T = triplet). Reprinted with permission from ref. 13. Copyright 2015 Royal Society of Chemistry.

The most efficient TTA-UC processes are usually carried out in solution phase because they allow fast diffusion of excited molecules. However, one of the key requisites of TTA-UC in solution is the anaerobic conditions of the reaction medium due to efficient triplet quenching by oxygen. Therefore, proper sealing of the reaction vessel must be ensured for TTA-UC in solution.²⁴ In order to block oxygen diffusion, TTA-UC process has been applied under aerated conditions by using different solid polymers or viscous liquids as support material.^{25,26,27} However, such solid polymer film or thick matrixes sometimes limit the diffusion of excited triplet molecules, requiring high-power incident photon source to maintain a certain concentration of excited triplet states. Therefore, development of new support materials that shows oxygen-blocking capability and simultaneously allows efficient TTA-UC of the incorporated donor/acceptor couple under low-power excitation appears to be a challenging task. In this context, employment of viscoelastic gel could fulfill the abovementioned criteria, opening a new research area to study the TTA-UC process for the different combinations of suitable donor and acceptor.

Simon *et al.* encapsulated Pd(II) mesoporphyrin IX and 9,10-diphenylanthracene (DPA) as UC chromophore pair into a DMF/DMSO based covalently crosslinked organogel prepared

from poly(vinyl alcohol) and hexamethylene diisocyanate (HMDI) (Figure 4).²⁸ The crosslinked organogel possessed good mechanical integrity, high molecular mobility, and high optical quality with a transmittance of above 95% in the visible range and additionally provided protection against triplet states quenching by oxygen. The UC quantum yield²⁹ increased from > 0.6 (under ambient conditions) to 14% (under oxygen-free conditions). Meanwhile, Schmidt *et al.* also reported TTA-UC in a supramolecular tetralin organogel made of 1,3:2,4-bis(3,4-dimethylbenzylidene) sorbitol (DMDBS) and containing palladium tetraphenylporfirin and DPA as UC pair.³⁰

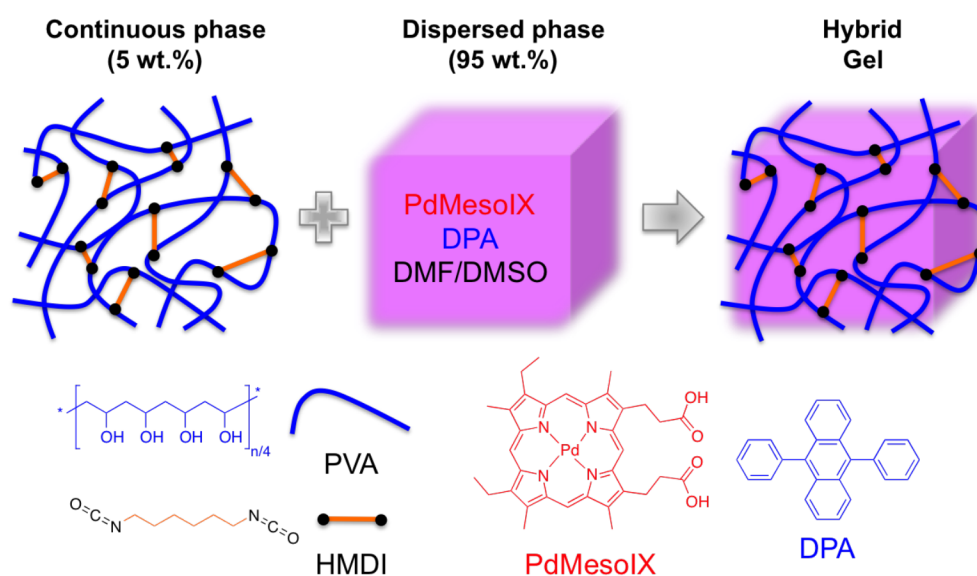
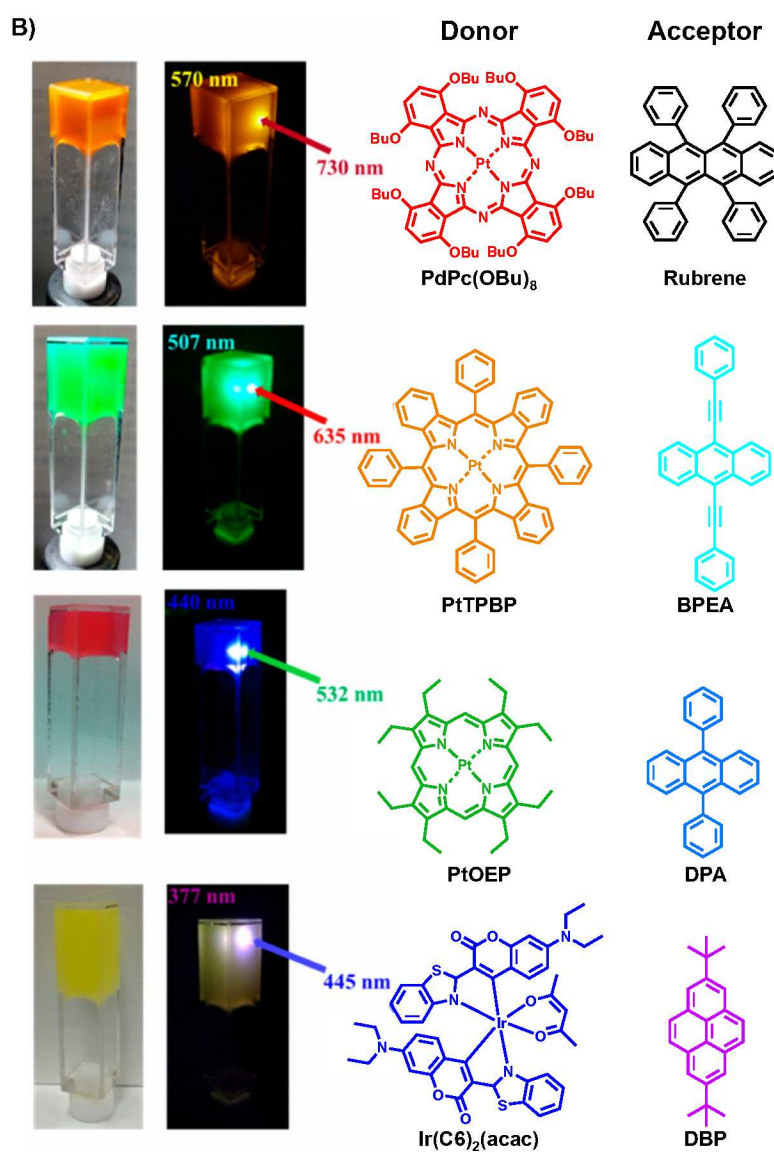
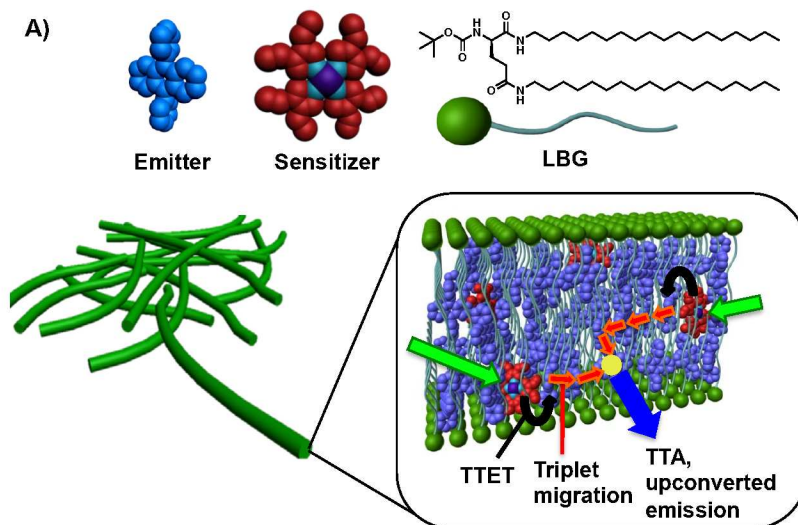


Figure 4. Graphic representation of the structure of the upconverting organogels studied and chemical structures of the constituents used. The photoactive material consists of a continuous polymer network and a liquid organic phase in which the upconverting chromophores are dissolved. Adapted with permission from ref. 28. Copyright 2015 Royal Society of Chemistry.

In the same year, Kimizuka *et al.* developed a very efficient TTA-UC process in a supramolecular organogel system under aerobic conditions and low-power excitation.³¹ *N,N'*-bis(octadecyl)-L-boc-glutamic diamide (LBG) was used as gel matrix, which can form a stable gel in a wide variety of polar and non-polar solvents due to the formation of hydrogen bond between the amide moieties and van der Waals interactions between the long aliphatic chains of

1
2
3 the gelator molecules (Figure 5A).³² The well-known bimolecular system consisting of PtOEP
4 (donor) and DPA (emitter) was chosen in this study as suitable TTA-UC pair.^{29,33} Excitation of
5 the PtOEP/DPA/LBG ternary gel system (air saturated state) with 532 green laser light caused an
6 upconverted emission at 435 nm, which was similar to that of DPA fluorescence when directly
7 excited with UV light (375 nm). A threshold excitation intensity of 1.48 mW cm^{-2} was observed
8 under aerobic conditions, lower than the solar irradiance of 1.6 mW cm^{-2} at $532 \pm 5 \text{ nm}$.
9 Interestingly, the intensity of DPA upconverted emission remained almost unchanged even after
10 exposure to air for 25 days. The upconversion quantum yield values under anaerobic and air-
11 saturated conditions were found to be 2.7% and 1.5%, respectively. Enhancement of the acceptor
12 concentration under air-saturated conditions gave rise to an increment in the upconversion
13 quantum yield value to ca. 3.5%. An exceptionally high oxygen blocking efficiency of 78% was
14 determined from the ratio between the measured lifetime of acceptor triplets for deaerated (228
15 ms) ternary gels and that for the air-saturated ternary gels. Additionally, the authors also showed
16 that UC emission intensity gradually decreased and reached an almost constant value above the
17 *gel-to-sol* transition. This fact was confirmed using the temperature-responsive nature of the
18 fibrous gel network. The disruption of the network upon increasing the temperature caused the
19 quenching of the excited triplet species due to dissolved oxygen. Furthermore, a few more
20 combinations of UC pairs were introduced into the supramolecular gel nanofibers, which enabled
21 some efficient near red-to-cyan, green-to-blue, IR-to-yellow and blue-to-UV wavelength
22 conversions (Figure 5B). Importantly, measurements of the diffusion constant of DPA triplets at
23 different temperatures, as well as studies in different solvents, confirmed a TTA mechanism
24 based on the triplet energy migration (TEM) in the supramolecular organized molecular
25 assembly. This concept involves the integration of donor molecules in the gel fibers (supported
26 by electron microscopy data) with densely accumulated acceptor molecules, where the excitation
27 of donor molecules is followed by donor-to-acceptor TTET, TEM through the acceptor arrays
28 and TTA of excited acceptors. In other words, a proximate preorganization of donor-acceptor
29 and acceptor-acceptor arrangements is crucial for favorable energy transfer processes and TEM
30 in the absence of free molecular diffusion. Such synergistic integration of donor-acceptor pairs
31 in nanofibrous aggregates has been identified as reminiscent of the biological photon-harvesting
32 apparatuses where excitation light energy is effectively harvested and converted in the array of
33 photosynthetic pigments embedded in the biomembranes.³¹

1
2
3
4
5
6
7
8
9
10
11
12
13
14
15
16
17
18
19
20
21
22
23
24
25
26
27
28
29
30
31
32
33
34
35
36
37
38
39
40
41
42
43
44
45
46
47
48
49
50
51
52
53
54
55
56
57
58
59
60



1
2
3 **Figure 5.** A) Schematic representation of the structural unit of the UC ternary gel system made
4 of a donor-acceptor pair and a LMW gelator, and proposed TEM mechanism occurring inside the
5 self-assembled gel fibers. B) Photographs of the UC co-gels in air-saturated DMF. Typical UC
6 pairs were used to form ternary gels allowing efficient (*from top to bottom*) near IR-to-yellow,
7 red-to-cyan, green-to-blue and blue-to-UV wavelength conversions. For all cases: [Donor] = 67
8 μM (except [PtOEP] = 33 μM); [acceptor] = 6.7 mM; [LBG] = 13.3 mM. Adapted with
9 permission from ref. 31. Copyright 2015 American Chemical Society.
10
11
12
13
14
15
16

17 The same research group also designed a novel amphiphilic acceptor molecule (Figure 6),
18 which contained a solvophobic multiple-amide-substituted 9,10-diphenylanthracene unit and
19 solvophilic alkyl chains, both units attached *via* a L-glutamate linker.³⁴ The presence of amide
20 bonds in the linker helped to promote crosslinking *via* hydrogen bonding among the networks
21 and also introduced chirality for better molecular orientation and thermal stability. When this
22 organogel was doped with PtOEP, an efficient TTA-UC with high UC quantum yield ($30 \pm 1\%$)
23 was obtained under ambient conditions. Interestingly, no upconverted emission was observed
24 from the frozen chloroform solution of DPA-PtOEP without the acceptor self-assembly at 77 K.
25 This can be explained because molecular diffusion is restricted at frozen conditions, resulting in
26 large intermolecular distance between chromophores and hence no energy migration and TTA
27 takes place. Additionally, different important materials such as gels and solid films made of
28 above-mentioned acceptor and donor were investigated as a TTA-UC system in the presence of
29 air demonstrating the versatility of the current design.³⁴
30
31
32
33
34
35
36
37
38
39
40
41
42
43
44
45
46
47
48
49
50
51
52
53
54
55
56
57
58
59
60

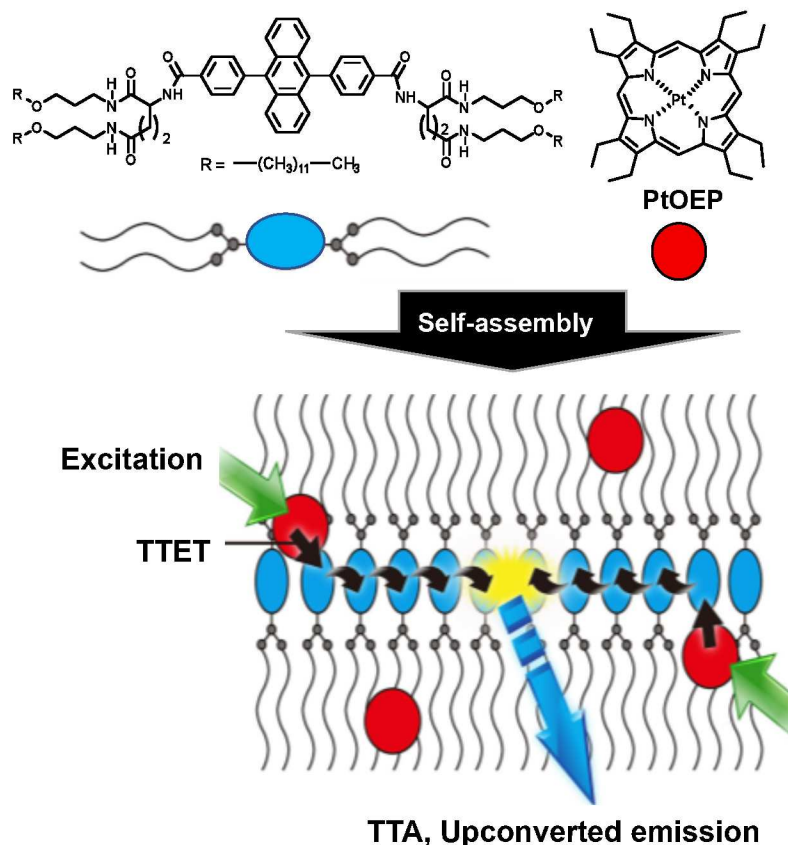


Figure 6. Schematic illustration of the basic self-assembly structure made of an amphiphilic acceptor molecule (*top-left*) in the presence of donor molecules (PtOEP), which bind to the self-assemblies by solvophobic interaction. Photoexcitation of donor molecules by green light induces donor-to-acceptor TTET, followed by TEM among the acceptor molecules, leading to efficient TTA and consequent upconverted blue emission. Adapted with permission from ref. 34. Copyright 2015 Nature Publishing Group.

Examples of TTA-UC in aqueous environments are scarce, essentially due to insolubility of chromophores and deactivation of excited triplets by dissolved oxygen molecules. In order to overcome these problems, Kimizuka *et al.* have very recently developed an air-stable photon upconverting hydrogel, which was formulated based on the concept of synergistic biopolymer-surfactant interactions.³⁵ The overall gel system consisted of gelatin, Triton X-100, sulfonated DPA (DPAS) as acceptor and PtOEP as a donor (Figure 7). They established that the non-polar surfactant domains constructed by definite organization of donor and acceptor chromophores, concomitantly shielded with dense gelatin hydrogen-bond networks prevented O₂ penetration in

the matrix. The UC efficiency was found to be 13.5%, which is to date the highest UC efficiency reported for air-saturated aqueous UC systems. Furthermore, the versatility of this strategy was demonstrated by studying the TTA-UC process in other biopolymers such as sodium alginate and agarose. Here, UC efficiencies were comparable to the gelatin based hydrogel. The use of biopolymer-based hydrogels as advanced light-harvesting systems opens some new potential applications in pharmaceutical, cosmetic, and detergent industries.

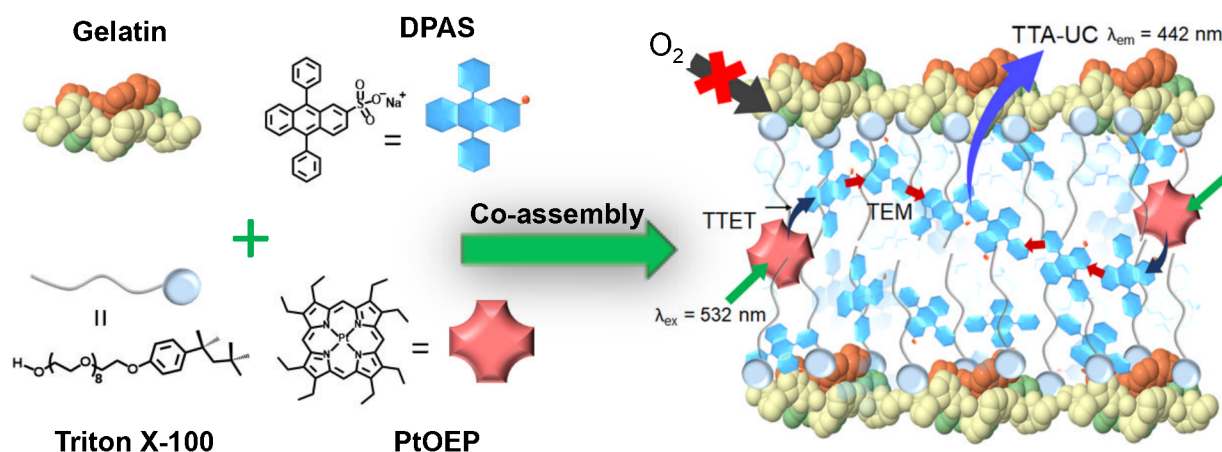


Figure 7. A schematic representation of G-TX-DPAS-PtOEP coassembly in photon upconverting hydrogel. Donor (PtOEP) and acceptor (DPAS) molecules are accumulated in the nonpolar domains of gelatin-TX100 hydrogel. The photoexcitation of donor is followed by a sequence of donor to-acceptor triplet–triplet energy transfer (TTET), triplet energy migration (TEM), triplet–triplet annihilation (TTA) among the acceptor molecules, and upconverted fluorescence from the acceptor excited singlet state. Adapted with permission from ref. 35. Copyright 2018 American Chemical Society.

PHOTOOXIDATION

In recent years, photooxidation processes inside nanoreactors such as micelles,³⁶ mesoporous molecular sieves,³⁷ oil-in-water emulsions,³⁸ among others, have attracted much attention due to the possibility of tailoring additional functionalities, organization and orientation of catalytic species, controllable molecular diffusion, large surface area to volume ratios, reduction of overheating/-concentration and the possibility of modeling and mimicking photoinduced processes in nature at the micron and submicron level.

1
2
3 Our research group studied for the first time the photooxidation of 1-(4-
4 methoxyphenyl)ethanol catalyzed by riboflavin tetraacetate (RFT) under air using visible light
5 inside different soft gel matrixes based on either LWM gelators or different biopolymers (Figure
6 8).³⁹ In this report, different approaches were adopted in order to achieve a tunable well-defined
7 nanoreactor. In the first approach, the catalyst was physically immobilized into several bio-based
8 polymers such as methylcellulose (**14**), κ -carrageenan (**15**), gelatin (**16**) and several LMW
9 gelators (Figure 8, compounds **5-12**) to investigate their possible effects on both selectivity and
10 reaction kinetics. Surprisingly, cyclohexane-based bis-amide based organogels made in CH₃CN
11 afforded full conversion (100 %) within 60 min in absence of thiourea (proton transfer agent) in
12 comparison with the solution phase where thiourea was needed to achieve 69 % conversion in
13 120 min. In addition, the kinetics of the photocatalytic process suggested a dependence between
14 the mechanical properties of the matrix and the efficiency of the reaction. For example, gels with
15 consisting of dense fibrillar networks and relatively high strength (confirmed from scanning
16 electron microscopy (SEM) and rheological measurements) usually showed the lowest reaction
17 rates. It is also worth mentioning that the chemical integrity and gelation propensity remained
18 unchanged even after several cycles of reuse. In comparison to this approach, the reaction rates
19 decreased significantly when other strategies were adopted to incorporate the photocatalyst into
20 the gel network, for example using a gelator molecule with covalently tethered photocatalyst or
21 employing a combination of photocatalyst and 6-methyl-1,3,5-triazine-2,4-diamine to form a
22 highly fluorescent H-bonded gelator. Overall, the results derived from this study supported the
23 existence of favorable interactions between gel fibers and substrates and/or catalyst.
24
25
26
27
28
29
30
31
32
33
34
35
36
37
38
39
40
41
42
43
44
45
46
47
48
49
50
51
52
53
54
55
56
57
58
59
60

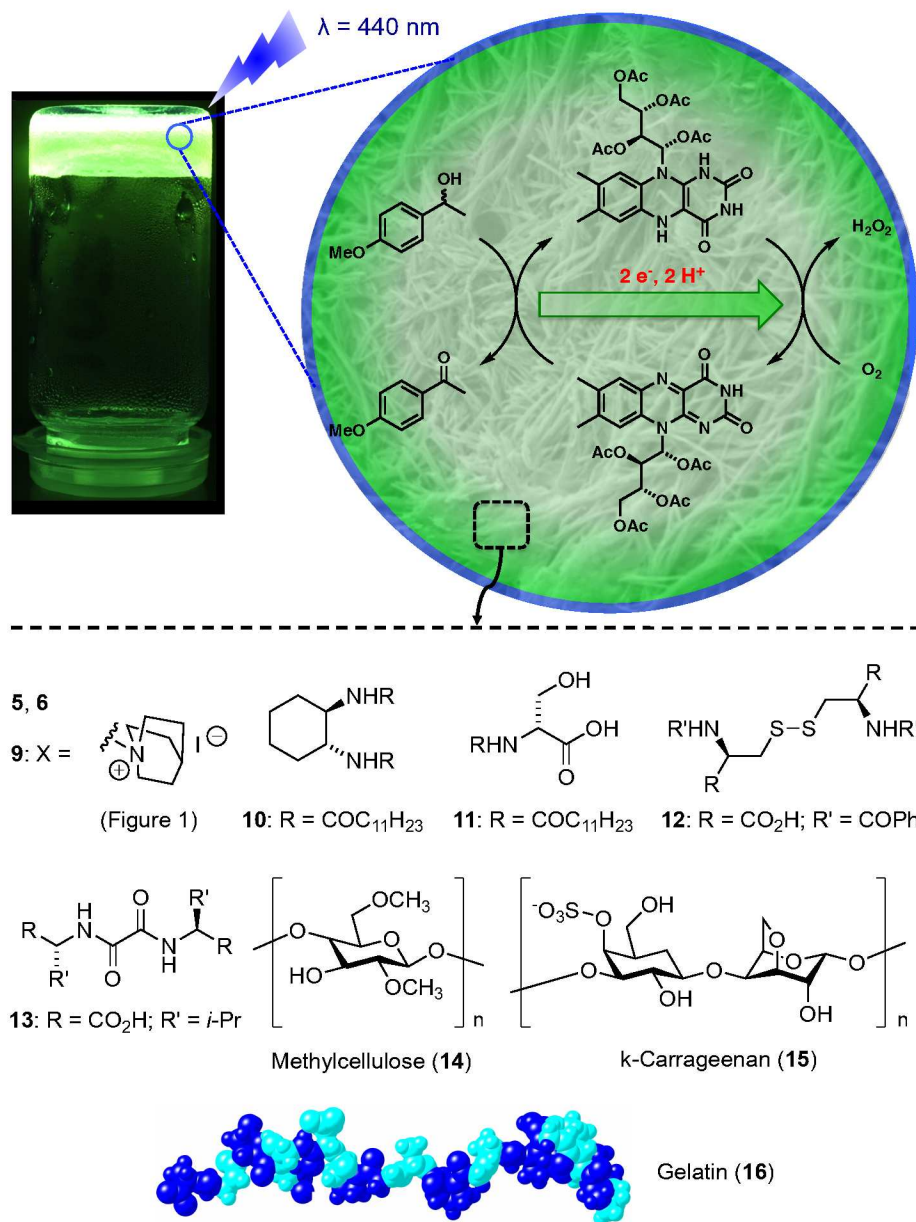


Figure 8. Illustration of riboflavin tetracetate-catalysed photooxidation of 1-(4-methoxymethyl)ethanol using blue visible light inside gel media (*top*) made of different types of gelators including low and high molecular weight compounds **5,6, 9-16** (*bottom*). Adapted with permission from ref. 39. Copyright 2013 Royal Society of Chemistry.

PHOTOREDUCTION

1
2
3 The photoreduction of aryl halides under mild conditions involving visible light as energy
4 source, room temperature, ambient pressure and air atmosphere is one of the most challenging
5 tasks in photoredox catalysis. The bond dissociation energy of PhBr ($BDE_{\text{PhBr}} = 3.6 \text{ eV}$) that is
6 significantly higher than the maximum energy of a single visible photon (3.1 eV) together with high
7 reduction potentials makes necessary the search for new activation methodologies. In this sense, TTA-
8 UC has been found to be a suitable tool for activating stable aryl halides under mild conditions in
9 solution.⁴⁰ Although hydrodebromination of aryl halides were successfully achieved, the general
10 method experienced low photocatalyst stability and oxygen-free atmosphere was a crucial
11 requirement. In order to overcome these limitations, we envisioned LMW organogels as suitable
12 confining media for such photoreactions under milder conditions. Thus, we reported the first intragel
13 photoreduction of aryl halides via a TTA mechanism. The gel network provided a stable
14 microenvironment for the challenging multi-step process under aerobic conditions, room
15 temperature and without additional additives. Specifically, intragel photoreductions of aryl
16 halides in air were investigated using PtOEP (sensitizer)-DPA (emitter) pair in supramolecular
17 gel networks made of *N,N'*-bis(octadecyl)-*L*-*boc*-glutamic diamide (**G-1**) or *N,N'*-((1*S*,2*S*)-
18 cyclohexane-1,2-diyl)didodecanamide (**G-2**).⁴¹ Photoreduction of 4-bromoacetophenone to
19 acetophenone catalyzed by the TTA-UC system was achieved after 2 h laser irradiation at 532
20 nm, yielding 58.2% of the desired product and nearly quantitative mass balance (Figure 9A).
21 Interestingly, the success of this approach was also perceptible to the naked eye. When the
22 reaction was performed in aerated DMF, complete decolorization of the original pink solution
23 was observed after irradiation due to decomposition of PtOEP by diffused molecular oxygen. On
24 the contrary, there was no change in the pink color in gel phase, supporting the hypothesis of an
25 efficient confinement effect of the gel network, preventing any quenching of the excited species
26 by dissolved oxygen (Figure 9B). Importantly, the results obtained in aerobic gel phase were
27 comparable to those obtained in solution under strict inert atmosphere. Furthermore, rheological
28 measurements of the gel matrix before and after laser irradiation demonstrated also the
29 preservation of the gel integrity in terms of thermal and mechanical properties.
30
31
32
33
34
35
36
37
38
39
40
41
42
43
44
45
46
47
48
49
50
51
52
53
54
55
56
57
58
59
60

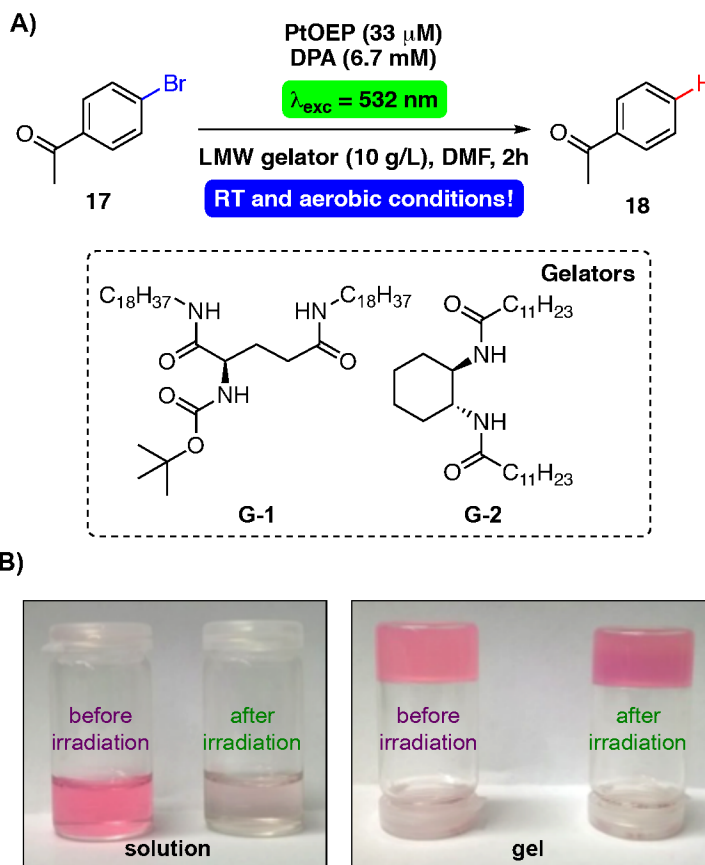


Figure 9. A) Scheme of photoreduction of 4-bromoacetophenone performed in gels made of LMW gelators **G-1** and **G-2**. B) Photographs of doped solutions before/after irradiation showing decolorization caused by degradation of PtOEP (*left*), and photographs of doped gel before/after irradiation (*right*). Adapted with permission from ref. 41. Copyright 2015 Royal Society of Chemistry.

A series of control experiments supported a reaction mechanism depicted in Figure 10. The intragel photoreduction of aryl halides takes place by successive TTA, single electron transfer (SET) and H-atom transfer (HAT) processes. The green-to-blue conversion begins with the selective irradiation at 532 nm of the sensitizer PtOEP. Then, after fast ISC the PtOEP triplet, $^3(\text{PtOEP})^*$, is efficiently quenched by DPA through triplet-triplet energy transfer (TTET) to generate long-lived DPA triplets, $^3(\text{DPA})^*$, and restoring PtOEP. Then, triplet energy migration (TEM) through the acceptor arrays in the supramolecular gel network induces the annihilation of $^3(\text{DPA})^*$ molecules affording the upconverting fluorescence $^1(\text{DPA})^*$. These species then induce

SET to the electrophilic aryl halides, forming the unstable radical anions $\text{ArX}^{\bullet-}$, which in turn undergo fragmentation into the corresponding aryl radicals Ar^{\bullet} and anions X^- . Finally, the product Ar-H is generated in a reduction reaction through rapid HAT from DMF. Oxidation of the resultant DMF^{\bullet} radical occurs by an exergonic back-electron transfer (BET), regenerating DPA and leading highly electrophilic DMF^+ species, which are further hydrolyzed into volatile products upon workup. Control experiments in non-proton donor solvents such as benzene showed no conversion of the starting material, thus discarding the possibility of Ar^{\bullet} trapping by gelator molecules through N-H abstraction.

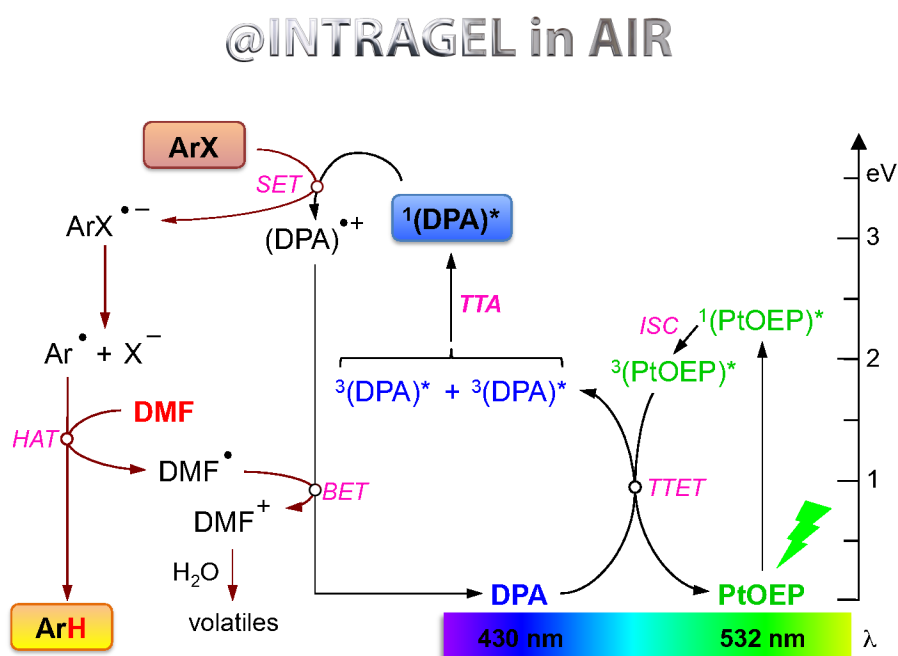


Figure 10. Plausible mechanism for visible light photoreduction of aryl halides at RT in air based on the combination of TTA-UC, SET and HAT processes inside the gel medium shown in Figure 9. Reprinted with permission from ref. 41. Copyright 2015 Royal Society of Chemistry.

Interestingly, all the foregoing learning can be applied to other challenged air-sensitive photo-redox catalytic reactions involving C-C bond formation. Very recently, our group has reported the proof of concept⁴² achieving selective functionalization of aryl halides using rhodamine-6G (Rh-6G)⁴³ as a photocatalyst under aerobic conditions in gel media, affording the desired products in comparable results to those obtained under strict inert conditions. The reaction is based on the application of different colours of visible light, which allows tuning the

1
2
3 redox potential of Rh-6G. For example, the ground state of the Rh 6G radical anion (Rh-6G \bullet^-)
4 formed upon photo-irradiation under green-light irradiation in the presence of an electron donor
5 (e.g. DIPEA) has a reduction potential of -1.0 V vs. SCE. However, subsequent irradiation of
6 Rh-6G \bullet^- with blue light generates the corresponding excited radical anion (Rh-6G \bullet^-*), which
7 displays a reduction potential of -2.4 V vs. SCE. As molecular oxygen quenches very efficiently
8 the excited states of the Rh-6G radical anions (Rh-6G \bullet^-*), an oxygen-free environment has been
9 strictly required to carry out these reactions. We demonstrated that this practical limitation can
10 be easily overcome replacing solution by a viscoelastic gel medium upon addition of a certain
11 amount of LMW gelator into the reaction mixture.
12
13
14
15
16
17
18

19 Initially, the reaction was carried out by using 2-bromobenzonitrile (**1**) as test substrate,
20 *N*-methylpyrrole (**25**) as trapping agent, Rh-6G as photocatalyst, *N,N'*-diisopropylethylamine
21 (DIPEA) as electron donor, *N,N'*-bis(octadecyl)-*L*-Boc-glutamic diamide (**G-1**) as gelator, and
22 DMSO as solvent (Figure 11). The reaction carried out in aerated DMSO solution at room
23 temperature under blue LED irradiation resulted in very low yield (5%) of the desired coupling
24 product. In sharp contrast, when the same reaction was carried out in presence of **G-1** gelator the
25 yield of the reaction significantly increased to 53%. The yield of the reaction can be improved
26 further by increasing the concentration of **G-1** (15 g/L), and the amount of DIPEA with respect
27 to reactant molecule. The use of other LMW gelators such as (*S,S*)-dodecyl-3-[2(3-dodecyl-
28 ureido)cyclohexyl]urea or *N,N'*-((1*R*,2*R*)-cyclohexane-1,2-diyl)didodecanamide, provided
29 comparable results during the photoredox reductive arylation with slight differences in their final
30 yields. Nevertheless, when 1,3:2,4-bis(3,4-dimethylbenzylidene)-sorbitol was used as a gelator,
31 the formation of the reduction byproduct was totally suppressed. Detailed reaction kinetics data
32 supported the effect of the gel network on the reaction rates. In addition, when 1,4-dibromo-2,5-
33 difluorobenzene was irradiated with green light ($\lambda_{\text{Ex}} = 530 \pm 15 \text{ nm}$) in the presence of Rh-6G,
34 DIPEA and *N*-methylpyrrole, only the corresponding monosubstituted product was formed. The
35 monosubstituted derivative is the only product obtained since activation of the second bromide
36 substituents is not possible by Rh-6G (reduction potential of Rh-6G ca. -1.0V vs. SCE), even
37 with higher catalyst loading. In contrast, when the reaction was performed under blue light
38 irradiation, the significant increase of the reduction potential of Rh-6G \bullet^-* enabled the formation
39 of the disubstituted product in good yields (Figure 11C). Additionally, this light colour-guided
40 photocatalytic arylation can also be performed in a sequential manner in aerated gel media
41
42
43
44
45
46
47
48
49
50
51
52
53
54
55
56
57
58
59
60

(Figure 11C). At first the substrate ethyl 2-bromo-(4-bromophenyl)acetate (**39**), which have two different carbon-halogen bonds (i.e., benzylic and aryl), lead to dehalogenation at the benzylic position upon irradiation with green light, affording the corresponding product **40** in modest yield. Subsequent activation of the aryl-bromide bond of product **40** under blue-light irradiation enabled the formation of the desired product **42** in good yield. In contrast to the observations made with the intragel TTA-UC process, comparative SEM images of undoped gels, gels loaded with the corresponding photocatalyst, and gels loaded with the photocatalyst and substrates, before and after irradiation, indicated that the incorporation of the substrates caused apparently a higher impact on the fibrillar morphology of the xerogel network than the photocatalysts alone. These results suggested that in this scenario there is not a spontaneous incorporation of the photocatalyst inside the gel fibers. It is worth mentioning that the separation of the gelator in these reactions is achieved by simple dilution-filtration and/or column chromatography.⁴²

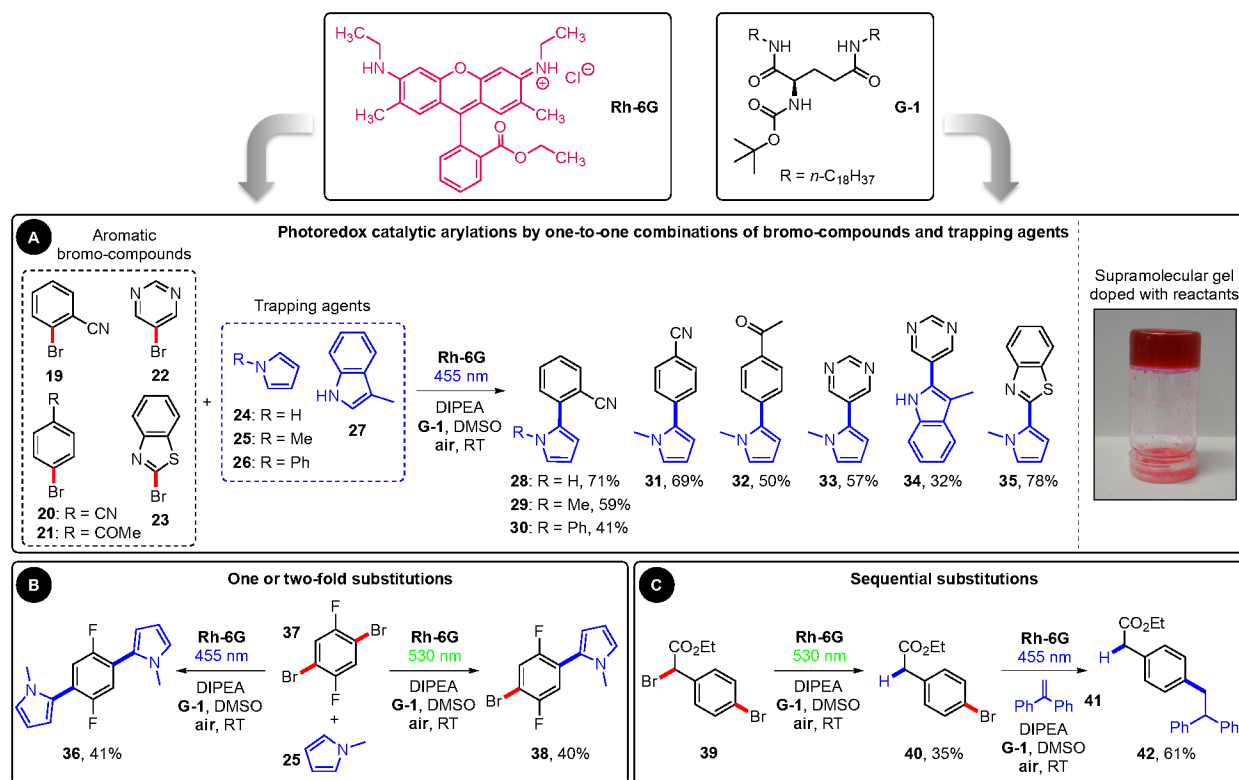


Figure 11. A) Substrate scope of intragel cross-coupling reactions between bromo compounds and trapping agents. Conditions: Bromo-compound **19-21** (0.1 mmol), trapping agent **24-27** (5-18 equiv), Rh-6G (15 mol%), DIPEA (2.2 equiv), **G-1** (15 g·L⁻¹), DMSO, air, RT, $\lambda_{\text{Ex}} = 455$

1
2
3 nm, reaction time: 24-96 h. Inset picture on the right: Typical appearance of a gel made of **G-1** in
4 DMSO loaded with catalyst, substrate and DIPEA. B) Chromoselective one- or two-fold
5 substitution reactions. C) Sequential substitution reactions. All yields correspond to isolated
6 products. Adapted with permission from ref. 42. Copyright 2018 American Chemical Society.
7
8
9

10 11 12 TRIFLUROMETHYLATION

13
14 Fluorinated and trifluoromethylated compounds have become widespread and indispensable
15 drugs in our modern society.⁴⁴ The incorporation of fluorine atoms into drug candidates has
16 major effects on the physico-chemical and biological properties of the parent molecule. For
17 instance, the inductive effects of the trifluoromethyl-group enhance bioavailability by reducing
18 the basicity of neighboring amines.⁴⁵ In 2001, Macmillan *et al.* reported a photocatalytic method
19 to carry out the trifluoromethylation of a broad range of arenes and heteroarenes. This strategy is
20 based on the use of Ru(phen)₃Cl₂ as photocatalyst, which generates trifluoromethyl radicals
21 ($\bullet\text{CF}_3$) *via* concomitant reduction of triflyl chloride (TfCl) upon light irradiation ($\lambda_{\text{EX}} = 455 \pm 15$
22 nm).⁴⁶ The proposed mechanism suggests the formation of a cyclo-hexadienyl radical from the
23 corresponding arene, which generates a cyclohexadienyl cation upon oxidation. Finally,
24 deprotonation of the cyclohexadienyl cation takes place in the presence of K₂HPO₄, leading to
25 the formation of the targeted trifluoromethyl arene. As this method also requires a strict inert
26 oxygen-free atmosphere, we recently optimized different gel formulations to carry out
27 trifluoromethylation of arenes under aerobic conditions.⁴² Specifically, a series of electron-rich 5-
28 membered heteroarenes (**25**, **43-46**) and also electron-deficient 6-membered heteroarenes (**50-52**)
29 were transformed to the targeted products in the presence of **G-1** gelator (Figure 12) under
30 aerated conditions in reasonable yields compared to those obtained in solution under an inert
31 atmosphere. Furthermore, when the same reaction proceeded in solution in the presence of
32 gelator **G-1** at a concentration marginally below the critical gelation concentration (CGC), the
33 final obtained product yields were ~10–15% lower compared to the reaction carried out in gel
34 phase at a concentration above the CGC. This makes sense if we consider that the oxygen-
35 blocking efficiency is achieved with the gel network is fully developed (i.e. above the CGC).
36 However, the product formation under these conditions supports the existence of intermolecular
37 interactions within some domains of the gel network and/or a beneficial effect of the enhanced
38 viscosity reducing the oxygen diffusion. The latter was also supported by the formation of the
39
40
41
42
43
44
45
46
47
48
49
50
51
52
53
54
55
56
57
58
59
60

1
2
3 reaction product in aerated frozen solution, albeit in ca. half yield compared to that observed in
4 gel at room temperature. Apparently, even a non-fully meshed network may offer some
5 interfaces to protect against oxygen deactivation compared to bulk solution. Interestingly, a
6 series of detailed kinetic and spectroscopic studies under different conditions indicated that in
7 this case the photocatalyst is not effectively shielded inside gel nanofibers from dissolved
8 oxygen. Contrary to the observations made in TTA-based reactions, the results of this study
9 indicated that the photocatalyst undergoes oxygen quenching as it is dissolved in the solvent pools
10 trapped in between the gel nanofibers. In this situation, and in contrast to free diffusion in
11 solution, the oxygen initially trapped in the gel –which has been proven to be still reactive–
12 should go through numerous entangled fibers to quench active species compartmentalized in
13 other solvent pools. In addition, although local consumption of dissolved oxygen could
14 potentially occur during photoirradiation, its effect has not been observed in phosphorescence
15 decay curves. Moreover, the gel network slows down significantly the diffusion of external
16 oxygen through the gel-air interface, thus preventing a fast deactivation of excited species
17 generated after the initial photoexcitation of the catalyst.
18
19
20
21
22
23
24
25
26
27
28
29
30

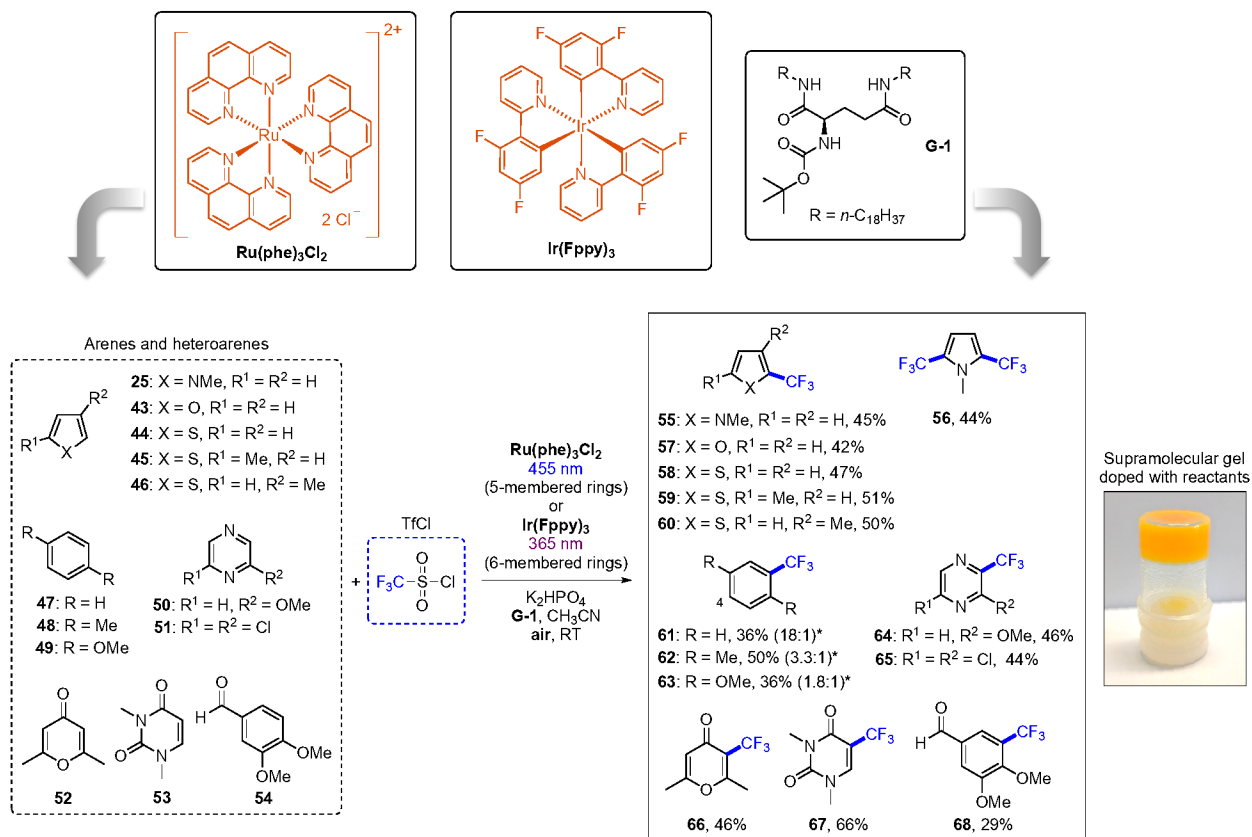


Figure 12. Substrate scope of intragel trifluoromethylation of 5- and 6-membered (hetero)arenes with TfCl. Conditions: (hetero)arene **25**, **43–54** (0.25 mmol), TfCl (2–4 equiv), photocatalyst (Ru(phen)₃Cl₂ (for 5-membered rings) or Ir(Fppy)₃ (for 6-membered rings) (catalyst loading: 1 mol% for 5-membered heteroarenes and 6-membered arenes; 2 mol% for 6-membered heteroarenes), K₂HPO₄ (3 equiv), **G-1** (10 g·L⁻¹), 2.5 mL MeCN, air, RT, λ_{EX} = 455 ± 15 nm (for (Ru(phen)₃Cl₂) or 365 nm ± 15 nm (for Ir(Fppy)₃), reaction time = 24–48 h. Picture on the right: Typical appearance of a gel made of **G-1** in MeCN loaded with Ru(phen)₃Cl₂/Ir(Fppy)₃, substrate, and K₂HPO₄. Reprinted with permission from ref. 42. Copyright 2018 American Chemical Society.

Recently, Li and co-workers described a metal-free strategy for trifluoromethylation of unactivated six-membered (hetero)arenes under UV or visible light irradiation.⁴⁷ In this method, sodium triflinate (CF₃SO₂Na, Langloies reagent) acts as a source of trifluoromethyl radicals (•CF₃) and diacetyl as a radical initiator, also requiring an inert atmosphere. We have recently described our preliminary results regarding a similar trifluoromethylation reaction of unactivated six-membered (hetero)arenes reaction under aerobic conditions using supramolecular gels as confining media.⁴⁸ When the reaction was performed under inert atmosphere conditions with vigorous stirring the overall yield was 96% favoring the monosubstituted product (i.e. monosubstituted 79%, disubstituted: 17%, Figure 13). The overall yield decreased to only 37% when the reaction was carried out under aerobic conditions. However, when the same reaction was performed in gel matrix under aerobic conditions the overall yield increased to 85%. It is worth mentioning that the yields and selectivity of this process are governed by several variables such as use of different light sources, LMW gelators (**G1-G4**, Figure 13) and gelator concentration. For instance, a maximum amount of monosubstituted product **2** (93%) was obtained when the gelator **G-1** was used at a concentration of 25 g L⁻¹, and provided full conversion with a percentage ratio 2:3 > 13:1. This was ascribed to the faster rate of oxygen diffusion below the optimal gelator concentration leading to the quenching of excited state intermediates, which cause a decrease in the overall reaction yield. Similarly, above the optimal concentration of the gelator the diffusion of reactants molecules into the gel matrix were restricted due to the compact nature of the reaction media causing a decrease in the overall product yield.

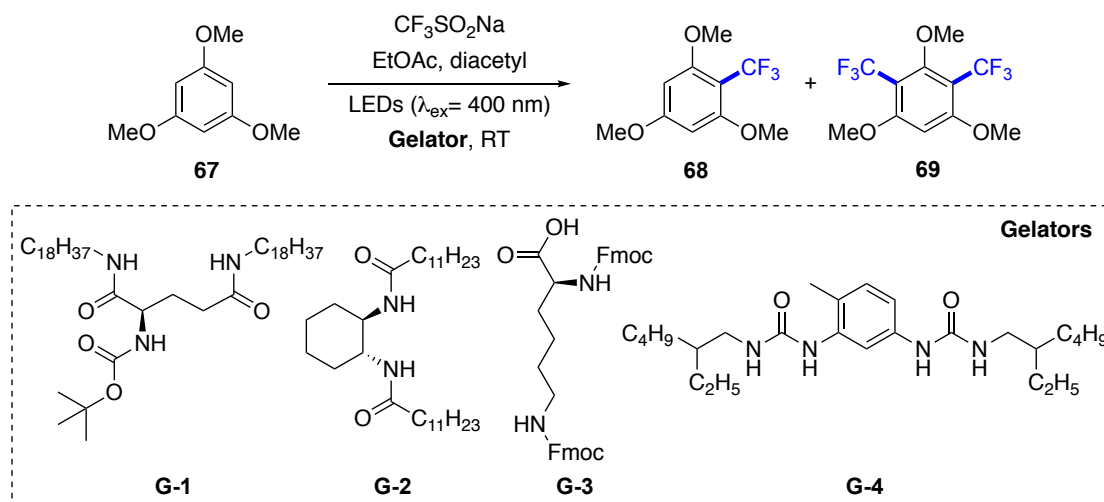


Figure 13. Model intragel photoinduced trifluoromethylation of 1,3,5-trimethoxy benzene **67** performed in gel media made using different LMW gelators (**G1-G4**).

CONCLUSION AND PERSPECTIVE

During the last few years, several groups have demonstrated the potential of gel networks as confining reaction media to perform photochemical processes under conditions milder than those required in homogeneous solution. Gel media has features that can be advantageous including, easy preparation and processability of the material, broad spectrum and rapid availability of gelator molecules, low gelator concentrations, large active surface areas and reversible stimuli-responsive nature, which is important for reutilization purposes. Apart from that, the photochemical reactions do not require any thermal trigger (that could lead to breakage of the gel matrix) to initiate reactions. In principle, confined spaces (e.g. solvent pools, inner part of the nanofibers) within the gel medium increase the local concentration of reactants and may positively influence the reaction outcome inside the soft nanoreactors through specific binding or interactions with gel fibers. Several photochemical reactions such as photo-dimerization, photo-oxidation, TTA-UC/SET-mediated photoreduction and trifluoromethylation reactions have been successfully carried out in gel media under aerobic conditions, affording the desired products in comparable yields to those obtained in homogeneous solution under rigorous inert conditions. Although this approach is just at its inception and additional fundamental studies are still required to establish the different kind of molecular interactions between reactants and gel

1
2
3 matrices, there is not doubt that non-conventional gel media can provide a versatile platform for
4 the discovery of new reaction pathways and facilitate the way that photochemical reactions are
5 traditionally carried out in academia and industry. The correct choice of gelators, reactants,
6 solvent and conditions for the assembly of these gelators is essential for controlling conversion,
7 kinetics and selectivity of intragel photo-induced reactions. In other words, fitting the reactant in
8 a specific alignment in the solvent pool of the gel matrix and making a specific reaction pathway
9 is a great and motivating challenge ahead for the scientific community. In addition, it is
10 important to carry out studies that will allow meaningful comparisons with other confined
11 systems. With remarkably similarities with the efficiency of biochemical reactions in confined
12 spaces (e.g. cell) under aerobic conditions, viscoelastic gel media seems to be a promising
13 candidate to facilitate important photochemical reactions under very mild conditions and
14 accelerate high-throughput screening of photocatalysts.
15
16
17
18
19
20
21
22
23
24

25 **Biographical Information**

26
27
28 **Binoy Maiti** received his Ph.D. in (2017) from the group of Prof. Priyadarsi De at the Indian
29 Institute of Science Education and Research Kolkata (India). He is now a postdoctoral fellow in
30 the group of Prof. David Díaz Díaz at the University of Regensburg (Germany), and his research
31 is focused on the development of polymeric functional materials.
32
33
34

35
36 **Alex Abramov** is a Ph.D. student in chemistry, advised by Profs. David Díaz Díaz and Oliver
37 Reiser at the University of Regensburg (Germany). His current interests are in the study of
38 photoinduced processes in confined microenvironments.
39
40

41
42 **Raúl Pérez-Ruiz** obtained his Ph.D. in chemistry (2006) under the guidance of Prof. Miguel A.
43 Miranda at the Polytechnic University of Valencia (UPV). Since 2007, he worked as
44 postdoctoral scientist in Athens, Cologne, Valencia and Regensburg. In 2017, he earned a Senior
45 Assistant Researcher position at IMDEA Energy Institute and currently he is Senior Researcher
46 at the UPV. He has been recipient of the AvHumboldt Fellowship, Juan de la Cierva, IEF Marie
47 Curie, Talent Attraction Program and CIDEAGENT. His actual research is focused on organic
48 photochemical processes and molecular spectroscopy
49
50
51
52
53
54
55
56
57
58
59
60

1
2
3 **David Díaz Díaz** earned his Ph.D. in chemistry (2002) under the supervision of Prof. Victor S.
4 Martín at the University of La Laguna (Spain). Then, he joined Prof. Finn's group as postdoc at
5 The Scripps Research Institute (San Diego, US). Since 2006, he has held various positions in
6 academia and industry. Among other scientific distinctions, he has received the DFG Heisenberg
7 Professorship in 2013, and the Young Investigator Award from the Polymer Network Group in
8 2014. Currently, he is a Privatdozent at the University of Regensburg (Germany) and a Tenured
9 Scientist at the Spanish National Research Council (CSIC) (Spain). He is also the Editor-in-Chief
10 of the journal *Gels*, and his main research interest focuses on the development of multifunctional
11 soft materials.
12
13
14
15
16
17
18
19

20 **ACKNOWLEDGMENTS**

21
22 The authors are grateful for the financial support from the University of Regensburg. R. P.-R.
23 thanks Valencian Community (grant No. CIDEAGENT/2018/044). D. D. D. thanks the DFG for
24 the Heisenberg Professorship Award.
25
26
27

28 **REFERENCES**

- 29
30
31 1 Otte, M. Size-Selective Molecular Flasks. *ACS Catal.* **2016**, *6*, 6491–6510.
32 2 Timmermans, S. B. P. E.; van Hest, J. C. M. Self-assembled nanoreactors based on peptides
33 and proteins. *Curr. Opin. Colloid Interface Sci.* **2018**, *35*, 26-35.
34 3 Nakamura, T.; Son, A.; Umehara, Y.; Ito, T.; Kurihara, R.; Ikemura, Y.; Tanabe, K. Confined
35 Singlet Oxygen in Mesoporous Silica Nanoparticles: Selective Photochemical Oxidation of
36 Small Molecules in Living Cells. *Bioconjugate Chem.* **2016**, *27*, 1058-1066.
37 4 Kagalwala, H. N.; Chirdon, D. N.; Mills, I. N.; Budwal, N.; Bernhard, S. Light-driven
38 hydrogen generation from microemulsions using metallosurfactant catalysts and oxalic acid.
39 *Inorg. Chem.* **2017**, *56*, 10162-10171.
40 5 Harris, C.; Kamat, P. V. Photocatalysis with CdSe nanoparticles in confined media: mapping
41 charge transfer events in the subpicosecond to second timescales. *ACS nano* **2009**, *3*, 682–690.
42 6 Limones-Herrero, D.; Pérez-Ruiz, R.; Jiménez, M. C.; Miranda, M. A. Retarded
43 Photooxidation of Cyamemazine in Biomimetic Microenvironments. *Photochem. Photobiol.*
44 **2014**, *90*, 1012-1016.
45
46
47
48
49
50
51
52
53
54
55
56
57
58
59
60

- 1
2
3
4
5
6
7
8
9
10
11
12
13
14
15
16
17
18
19
20
21
22
23
24
25
26
27
28
29
30
31
32
33
34
35
36
37
38
39
40
41
42
43
44
45
46
47
48
49
50
51
52
53
54
55
56
57
58
59
60
-
- 7 Bu, M.; Cai, C.; Gallou, F.; Lipshutz, B. H. PQS-enabled visible-light iridium photoredox catalysis in water at room temperature. *Green Chem.* **2018**, *20*, 1233-1237.
- 8 Wen, J.; Ma, C.; Huo, P.; Liu, X.; Wei, M.; Liu, Y.; Yao, X.; Ma, Z.; Yan, Y. Construction of vesicle CdSe nano-semiconductors photocatalysts with improved photocatalytic activity: Enhanced photo induced carriers separation efficiency and mechanism insight. *J. Environ. Sci.* **2017**, *60*, 98-107.
- 9 Askes, H. C.; Bahreman, A.; Bonnet, S. Activation of a Photodissociative Ruthenium Complex by Triplet-Triplet Annihilation Upconversion in Liposomes. *Angew. Chem. Int. Ed.* **2014**, *126*, 1047-1056.
- 10 Zhang, K.; Zhou, W.; Zhang, X.; Sun, B.; Wang, L.; Pan, K.; Jiang, B.; Tian, G.; Fu, H. Self-floating amphiphilic black TiO₂ foams with 3D macro-mesoporous architectures as efficient solar-driven photocatalysts. *Appl. Catal. B* **2017**, *206*, 336-343.
- 11 Ghasimi, S.; Prescher, S.; Wang, Z. J.; Landfester, K.; Yuan, J.; Zhang, K. A. I. Heterophase Photocatalysts from WaterSoluble Conjugated Polyelectrolytes: An Example of SelfInitiation under Visible Light. *Angew. Chem. Int. Ed.* **2015**, *54*, 14549-14553.
- 12 Yamanaka, M. Urea derivatives as low-molecular-weight gelators. *J. Incl. Phenom. Macrocycl. Chem.* **2013**, *77*, 33-48.
- 13 Pérez-Ruiz, R.; Díaz, D. D. Photophysical and photochemical processes in 3D self-assembled gels as confined microenvironments. *Soft Matter* **2015**, *11*, 5180-5187.
- 14 Shchukin, D.; Sviridov, D. Photocatalytic processes in spatially confined micro- and nanoreactors. *J. Photochem. Photobiol. C: Photochem. Rev.* **2006**, *7*, 23-39.
- 15 Maldotti, A.; Molinari, A.; Amadelli, R. Photocatalysis with Organized Systems for the Oxofunctionalization of Hydrocarbons by O₂. *Chem. Rev.* **2002**, *102*, 3811-3836.
- 16 Díaz, D. D.; Kühbeck, D.; Koopmans, R. J. Stimuli-responsive gels as reaction vessels and reusable. *Chem. Soc. Rev.* **2011**, *40*, 427-448, and references therein.
- 17 Chen, M.; Zhong, M.; Johnson, J. A. Light-Controlled Radical Polymerization: Mechanisms, Methods, and Applications. *Chem. Rev.* **2016**, *116*, 10167-10211.
- 18 Vriezema, D. M.; Aragoné's, M. C.; Elemans, J. A. A. W.; Cornelissen, J. J. L. M.; Rowan, A. E.; Nolte, R. J. M. Self-Assembled Nanoreactors. *Chem. Rev.* **2005**, *105*, 1445-1489.

- 1
2
3
4 19 Kaanumalle, L. S.; Ramamurthy, V. Photodimerization of acenaphthylene within a
5 nanocapsule: excited state lifetime dependent dimer selectivity. *Chem. Commun.* **2007**, 1062-
6 1064
7
8
9 20 Nakamura, Y.; Imakura, Y.; Kato, T.; Morita, Y. Reactions using micellar system:
10 photochemical dimerization of acenaphthylene. *J.C.S. Chem. Comm.* **1997**, 887-888.
11
12 21 Bhat, S.; Maitra, U. Hydrogels as Reaction Vessels: Acenaphthylene Dimerization in
13 Hydrogels Derived from Bile Acid Analogues. *Molecules* **2007**, *12*, 2181.
14
15 22 Dawn, A.; Fujit, N.; Haraguchi, S.; Sada, K.; Shinkai, S. An organogel system can control the
16 stereochemical course of anthracene photodimerization, *Chem. Commun.* **2009**, 2100-2102.
17
18 23 Vadrucci, R.; Monguzzi, A.; Saenz, F.; Wilts, B. D.; Simon, Y. C.; Weder, C. Nanodroplet-
19 Containing Polymers for Efficient Low-Power Light Upconversion. *Adv. Mater.* **2017**, *29*,
20 1702992.
21
22 24 Grewer, C.; Brauer, H.-D. Mechanism of the Triplet-State Quenching by Molecular Oxygen
23 in Solution. *J. Phys. Chem.* **1994**, *98*, 4230-4235.
24
25 25. Miteva, T.; Yakutkin, V.; Nelles G.; Balushev, S. Annihilation assisted upconversion: all-
26 organic, flexible and transparent multicolour display. *New J. Phys.* **2008**, *10*, 103002.
27
28 26. Simon Y. C.; Weder. C. Low-power photon upconversion through triplet-triplet annihilation
29 in polymers. *J. Mater. Chem.* **2012**, *22*, 20817-20830.
30
31 27 Lee, S. H.; Lott, J. R.; Simon, Y. C.; Weder. C. Melt-processed polymer glasses for low-
32 power upconversion *via* sensitized triplet-triplet annihilation. *J. Mater. Chem. C* **2013**, *1*, 5142-
33 5148.
34
35 28 Vadrucci, R.; Weder, C.; Simon, Y. C. Organogels for low-power light upconversion. *Mater.*
36 *Horiz.* **2015**, *2*, 120-124.
37
38 29 Yanai, N.; Kimizuka, N. New triplet sensitization routes for photon upconversion: thermally
39 activated delayed fluorescence molecules, inorganic nanocrystals, and singlet-to-triplet
40 absorption. *Acc. Chem. Res.* **2017**, *50*, 2487-2495.
41
42 30 Sripathy, K.; MacQueen, R. W.; Peterson, J. R.; Cheng, Y. Y.; Dvorak, M.; McCamey, D. R.;
43 Treat, N. D.; Stingelin, N.; Schmidt. T.W. Highly efficient photochemical upconversion in a
44 quasi-solid organogel. *Mater. Chem. C* **2015**, *3*, 616-622.
45
46
47
48
49
50
51
52
53
54
55
56
57
58
59
60

- 1
2
3
4 31 Duan, P.; Yanai, N.; Nagatomi, H.; Kimizuka, N. Photon Upconversion in Supramolecular
5 Gel Matrixes: Spontaneous Accumulation of Light-Harvesting Donor-Acceptor Arrays in
6 Nanofibers and Acquired Air Stability. *J. Am. Chem. Soc.* **2015**, *137*, 1887-1894.
7
8 32 Kira, Y.; Okazaki, Y.; Sawada, T.; Takafuji, M.; Ihara, H. Amphiphilic molecular gels from
9 x-aminoalkylated L-glutamic acid derivatives with unique chiroptical properties, *Amino Acids*
10 **2010**, *39*, 587-597.
11
12 33 Ye, C.; Zhou, L.; Wang, X.; Liang, Z. Photon upconversion: from two-photon absorption
13 (TPA) to triplet-triplet annihilation (TTA). *Phys.Chem.Chem.Phys.* **2016**, *18*, 10818-10835.
14
15 34 Ogawa T.; Yanai N.; Monguzzi A.; Kimizuka N. Highly Efficient Photon Upconversion in
16 Self-Assembled Light-Harvesting Molecular Systems. *Sci. Rep.* **2015**, *5*, 10882.
17
18 35 Bharmoria, P.; Hisamitsu, S.; Nagatomi, H.; Ogawa, T.; Morikawa, M.; Yanai, N.; Kimizuka,
19 N. Simple and Versatile Platform for Air-Tolerant Photon Upconverting Hydrogels by
20 Biopolymer-Surfactant-Chromophore Co-assembly, *J. Am. Chem. Soc.* **2018**, *140*, 10848-10855.
21
22 36 Hovey, M. C. Micellar Photochemistry. Photooxidations with Intracellular-Generated Singlet
23 Oxygen. *J. Am. Chem. Soc.* **1982**, *104*, 4196-4202.
24
25 37 Feng, K.; Zhang, R.-Y.; Wu, L.-Z.; Tu, B.; Peng, M.-L.; Zhang, L.-P.; Zhao, D.; Tung, C.-H.
26 Photooxidation of olefins under oxygen in platinum (II) complex-loaded mesoporous molecular
27 sieves. *J. Am. Chem. Soc.* **2006**, *128*, 14685-14690.
28
29 38 Kagalwala, H.N.; Chirdon, D.N.; Mills, I.N.; Budwal, N.; Bernhard, S. Light-driven hydrogen
30 generation from microemulsions using metallosurfactant catalysts and oxalic acid. *Inorg. Chem.*
31 **2017**, *56*, 10162–10171.
32
33 39 Bachl, J.; Hohenleutner, A.; Dhar, B. B.; Cativiela, C.; Maitra, U.; König B.; Díaz, D. D.
34 Organophotocatalysis in nanostructured soft gel materials as tunable reaction vessels:
35 comparison with homogeneous and micellar solutions. *J. Mater. Chem. A* **2013**, *1*, 4577-4588.
36
37 40 Majek, M.; Faltermeier, U.; Dick, B.; Ruiz, R.P.; Wangelin, A. J. v. *Chem. Eur. J.* **2015**, *21*,
38 15496-15501.
39
40 41 Häring, M.; Ruiz, R.P.; Wangelin, A. J. v.; Díaz, D. D. Intragel photoreduction of aryl halides
41 by green-to-blue upconversion under aerobic conditions. *Chem. Commun.* **2015**, *51*, 16848-
42 16851.
43
44
45
46
47
48
49
50
51
52
53
54
55
56
57
58
59
60

1
2
3
4 42 Häring, M.; Abramov, A.; Okumura, K.; Ghosh, I.; König, B.; Yanai, N.; Kimizuka, N.; Díaz,
5 D. D. Air-Sensitive Photoredox Catalysis Performed under Aerobic Conditions in Gel Networks.
6 *J. Org. Chem.* **2018**, *83*, 7928-7938.

7
8
9 43 Ghosh, I.; König, B. Chromoselective photocatalysis: Controlled bond activation through
10 light-color regulation of redox potentials. *Angew. Chem., Int. Ed.* **2016**, *55*, 7676-7679.

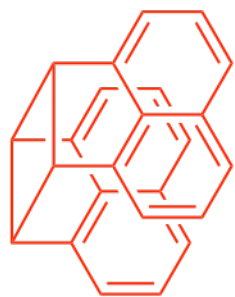
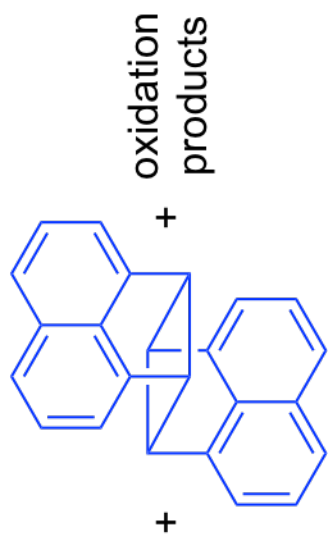
11
12
13 44 Zhou, Y.; Wang, J.; Gu, Z.; Wang, S.; Zhu, W.; Aceña, J. L.; Soloshonok, V. A.; Izawa, K.;
14 Liu, H. Next Generation of Fluorine-Containing Pharmaceuticals, Compounds Currently in
15 Phase II–III Clinical Trials of Major Pharmaceutical Companies: New Structural Trends and
16 Therapeutic Areas. *Chem. Rev.* **2016**, *116*, 422-518.

17
18
19 45 Müller, K.; Faeh, C.; Diederich F. Fluorine in Pharmaceuticals: Looking Beyond Intuition.
20 *Science* **2007**, *317*, 1881.

21
22
23 46 Nagib, D. A.; MacMillan, D. W. C. Trifluoromethylation of arenes and heteroarenes by
24 means of photoredox catalysis *Nature* **2011**, *480*, 224-228.

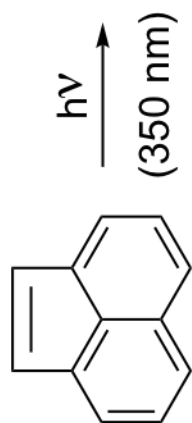
25
26
27 47 Li, L.; Mu, X.; Liu, W.; Wang, Y.; Mi, Z.; Li, C.J. Simple and clean photoinduced aromatic
28 trifluoromethylation reaction. *J. Am. Chem. Soc.* **2016**, *138*, 5809-5812.

29
30 48 Abramov, A.; Vernickel, H.; Saldías, C.; Díaz D. D. Metal- and Oxidant-Free Photoinduced
31 Aromatic Trifluoromethylation Performed in Aerated Gel Media: Determining the Effects on
32 Yield and Selectivity. *Molecules* **2019**, *24*, 29.

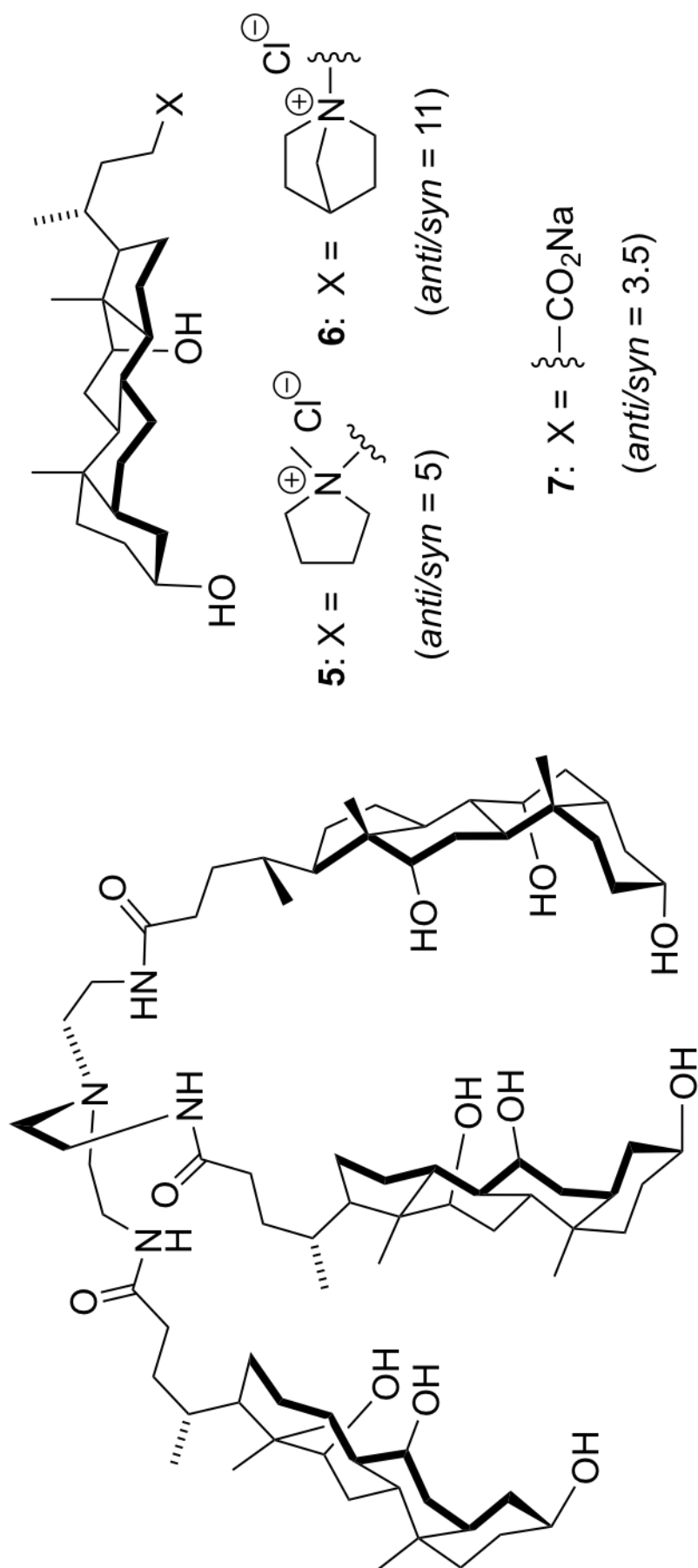


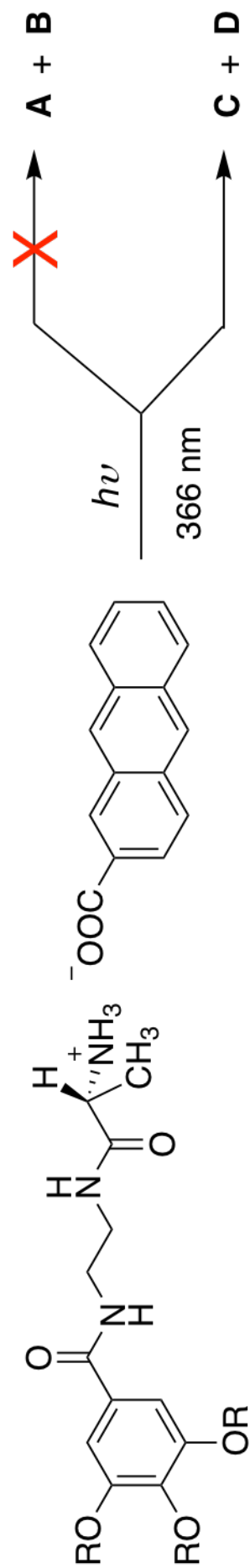
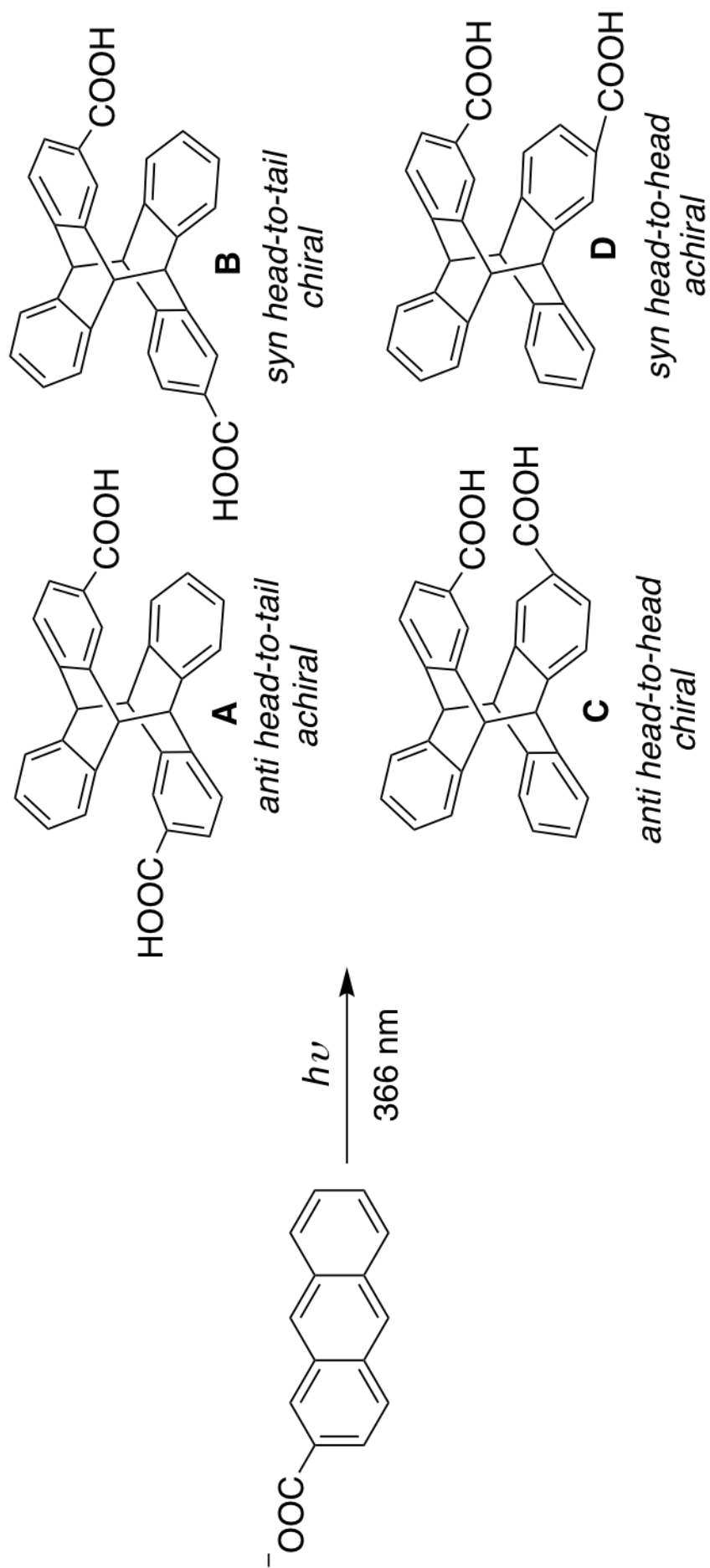
2 (*syn* dimer)

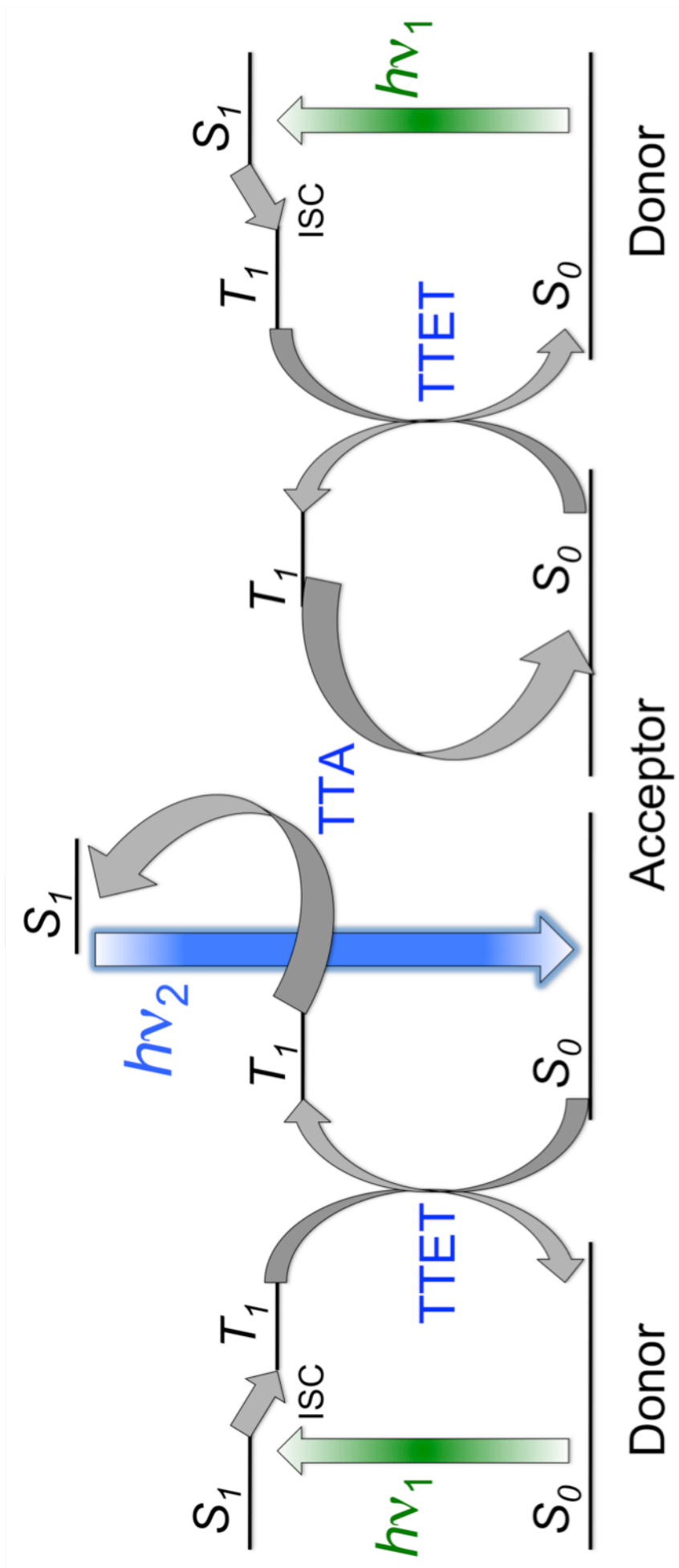
3 (*anti* dimer)

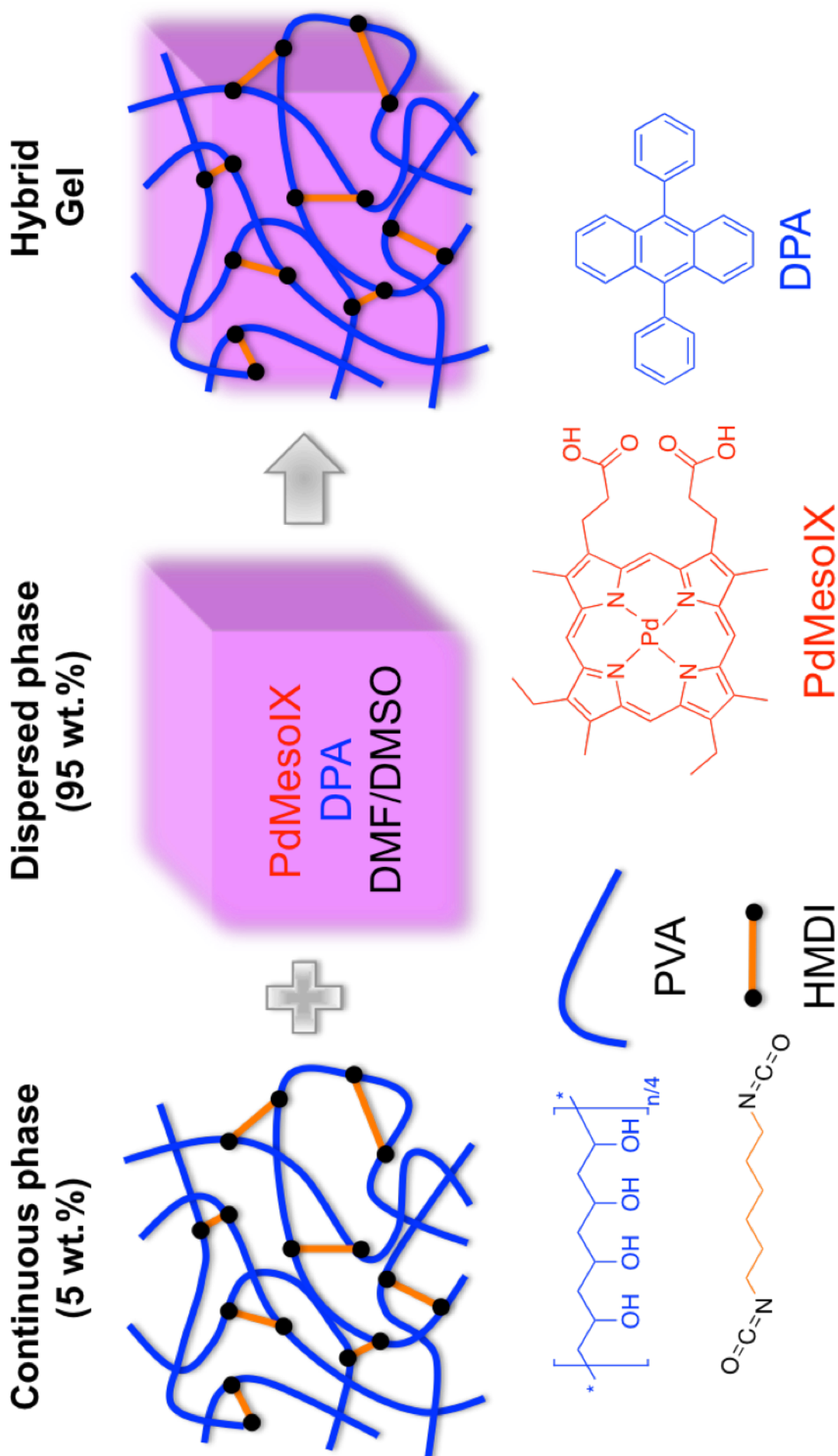


1





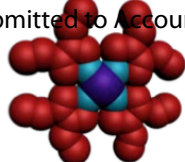




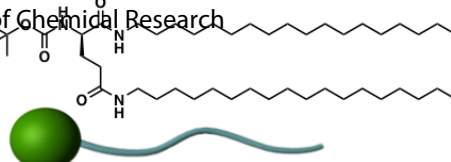
A)



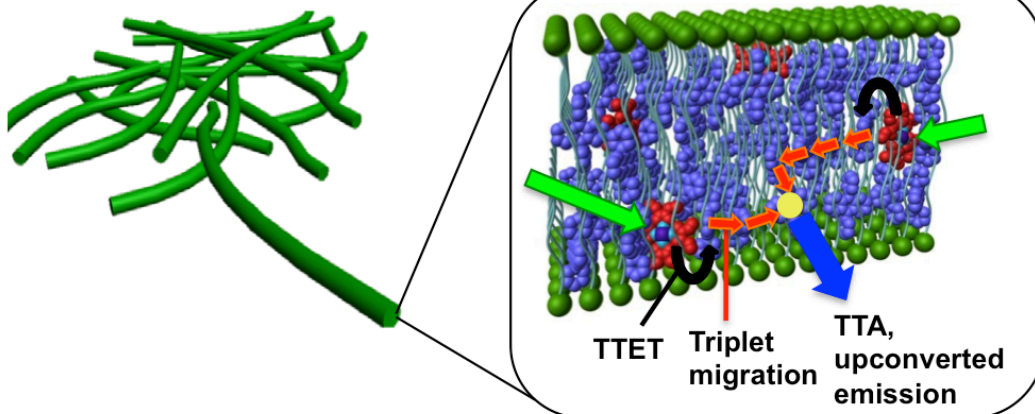
Emitter



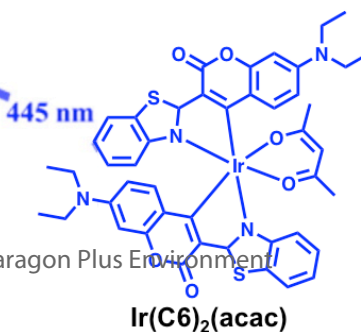
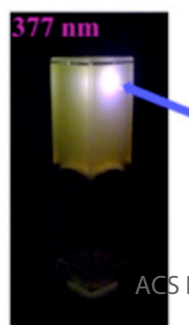
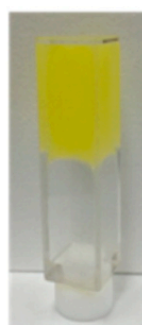
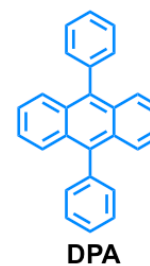
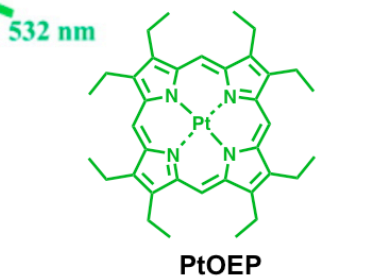
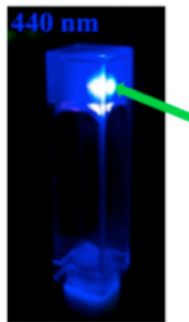
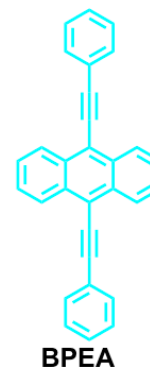
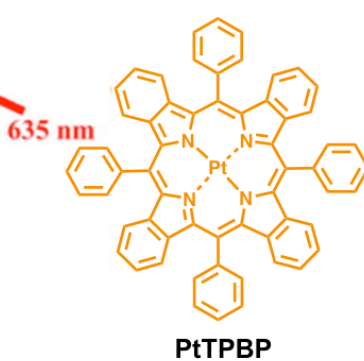
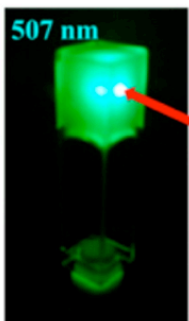
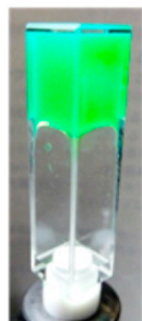
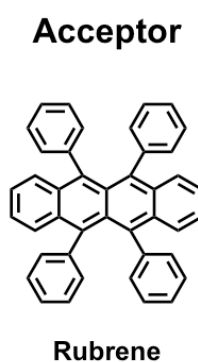
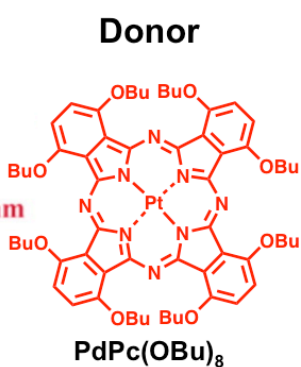
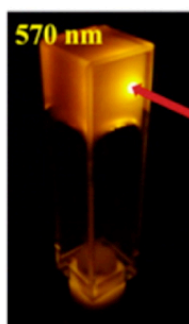
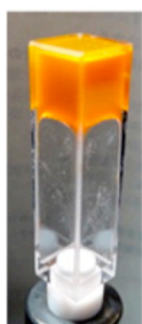
Sensitizer

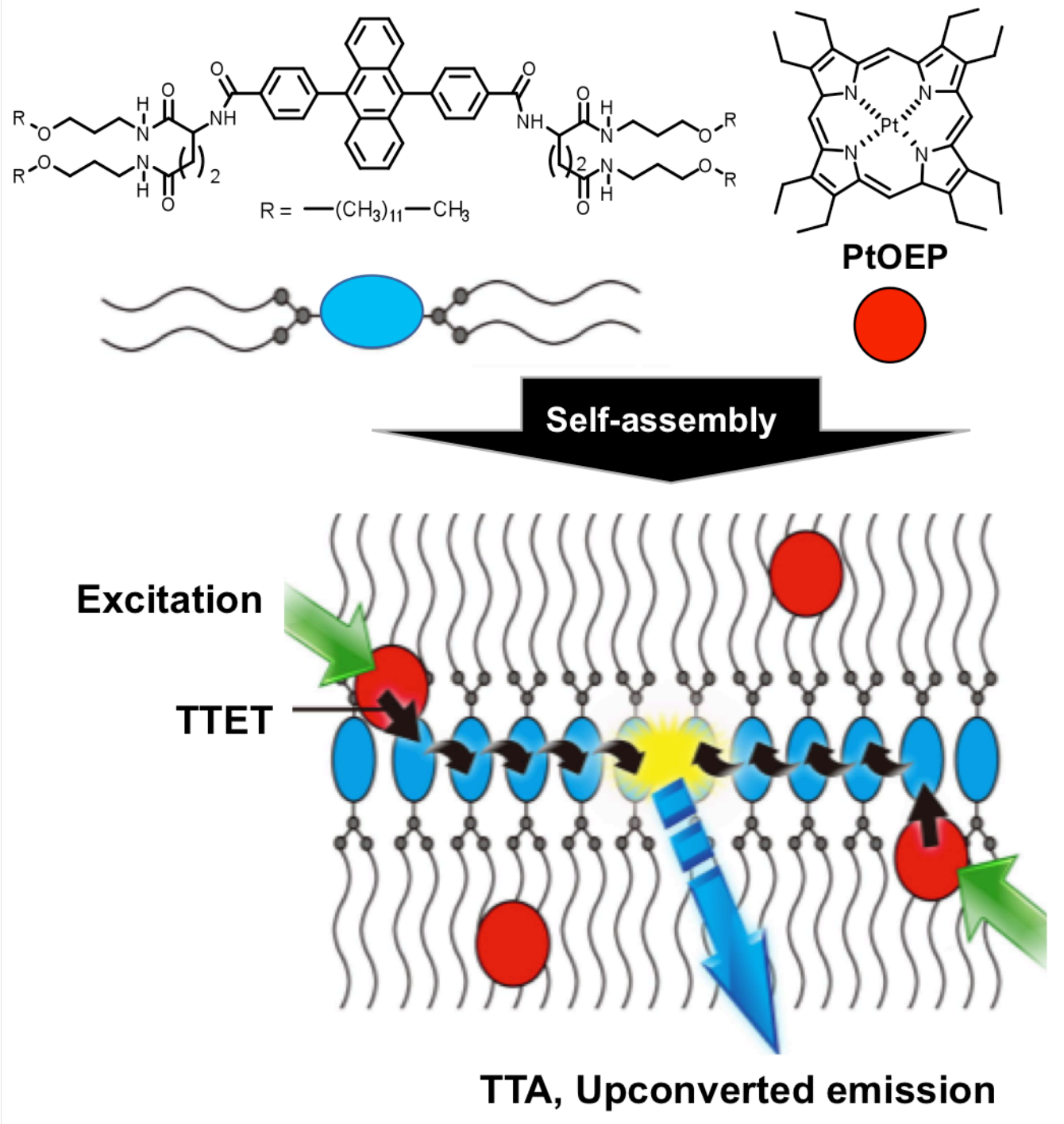


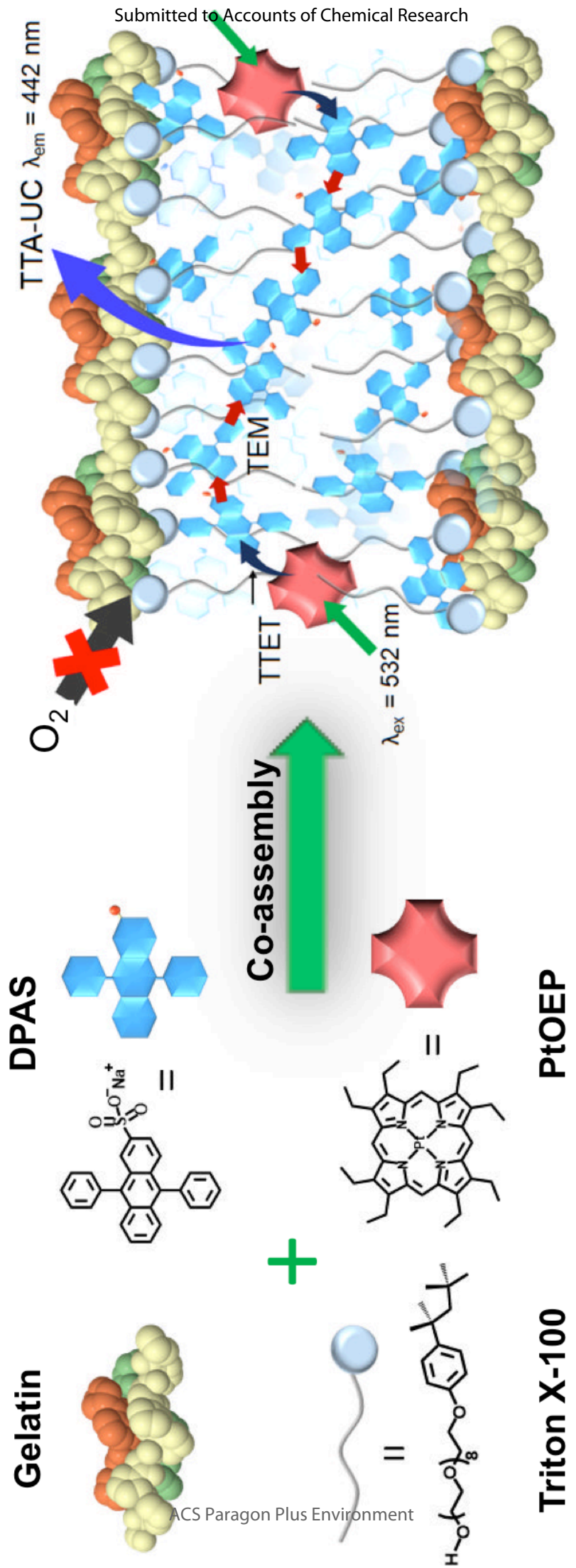
LBG

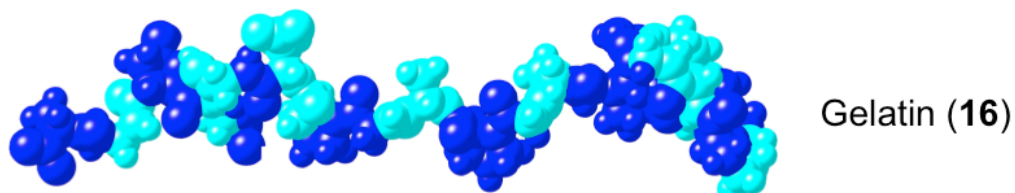
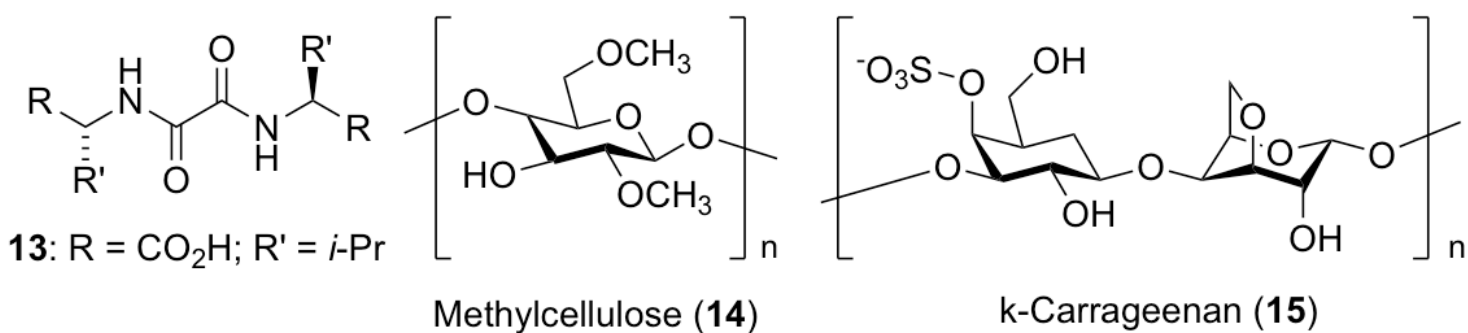
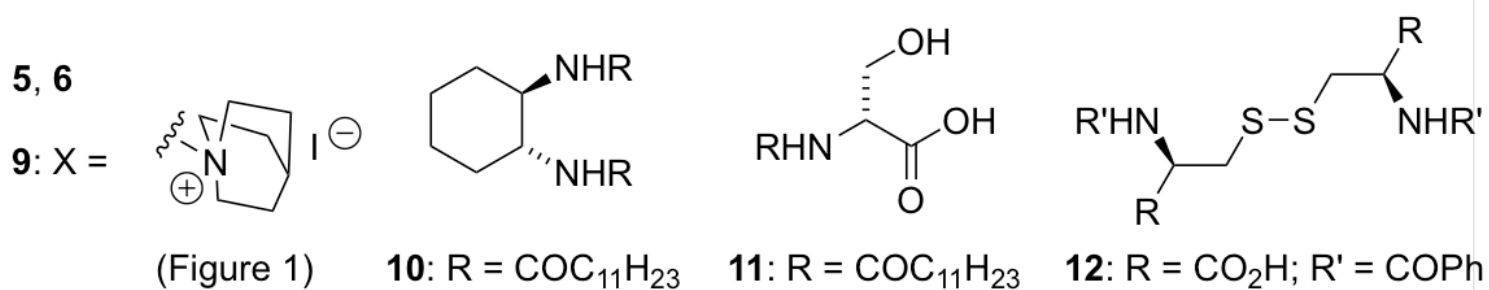
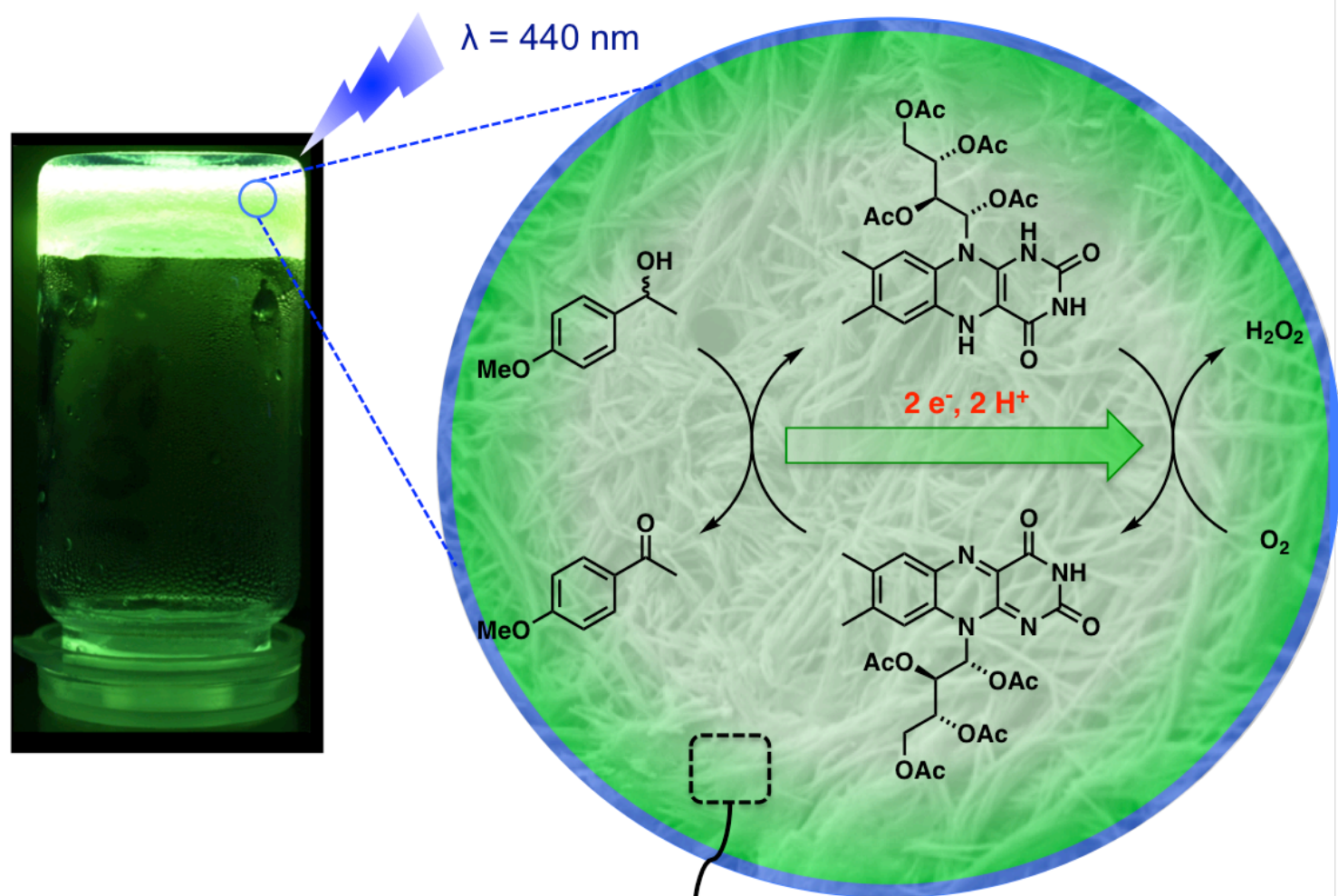


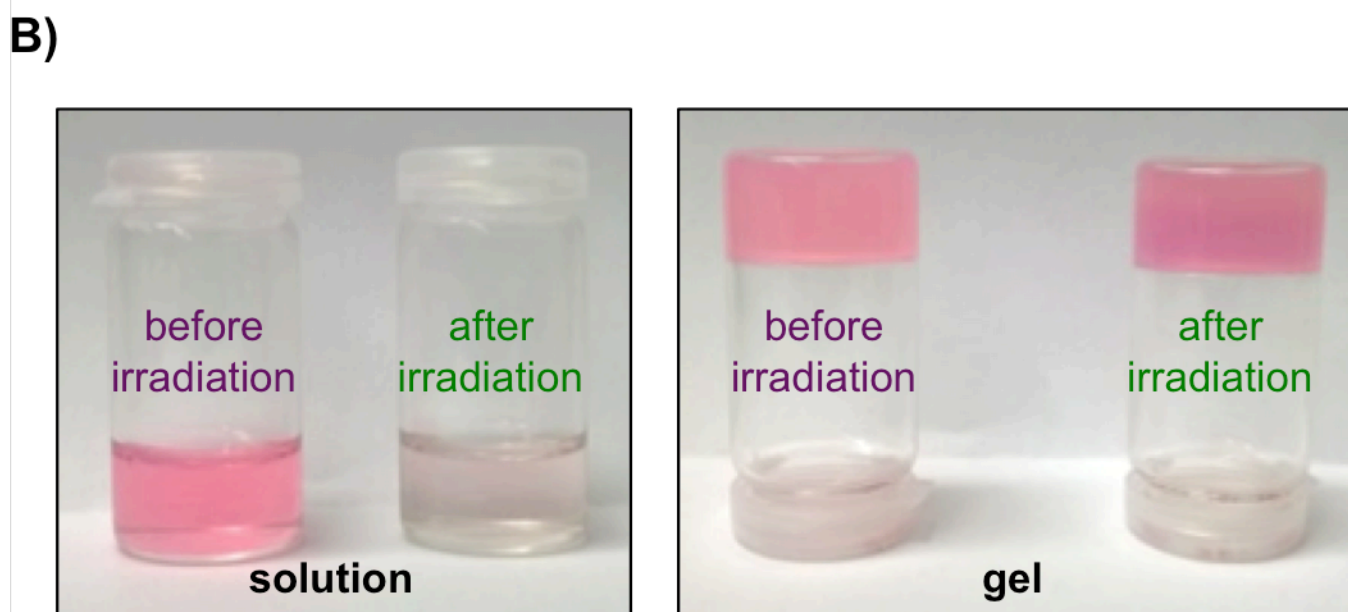
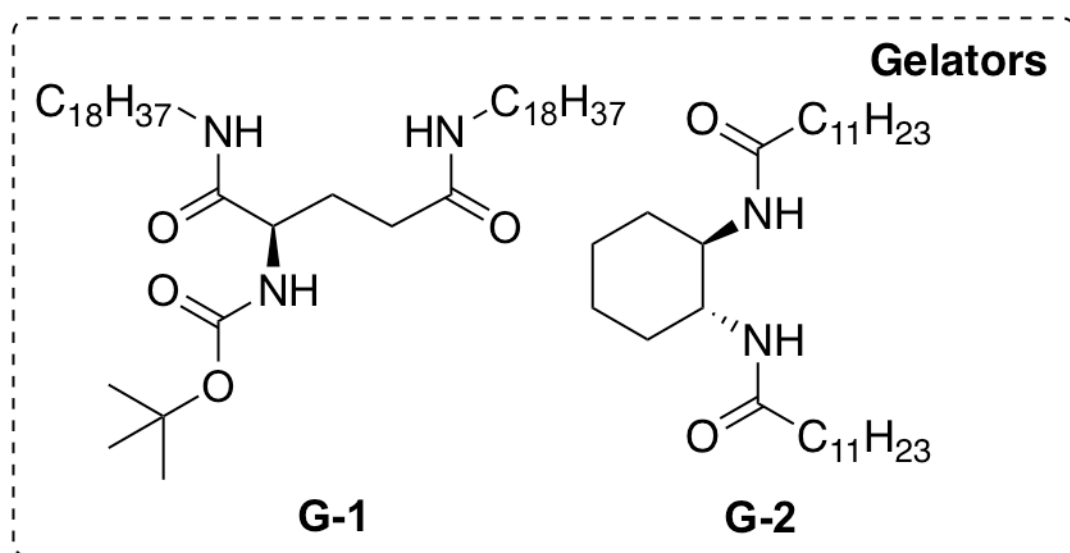
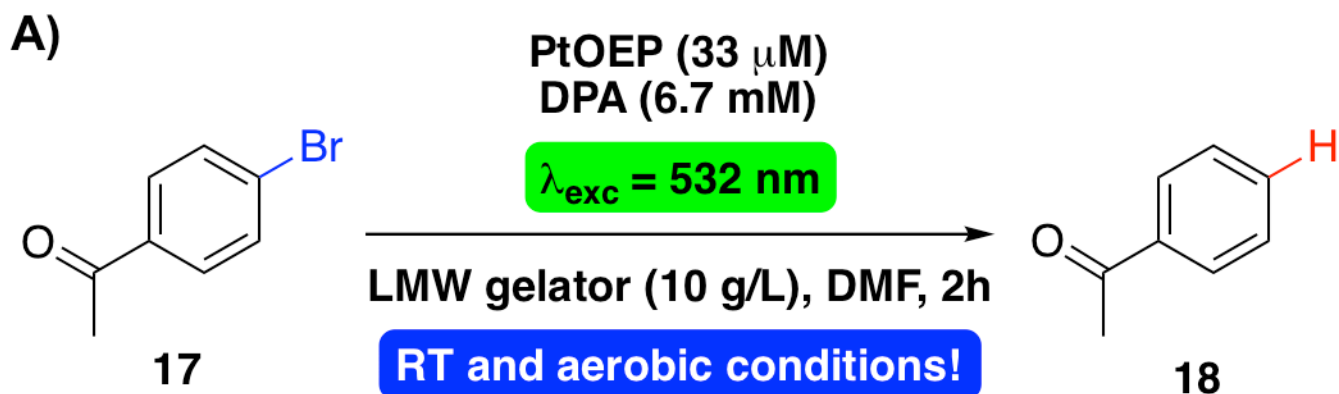
B)



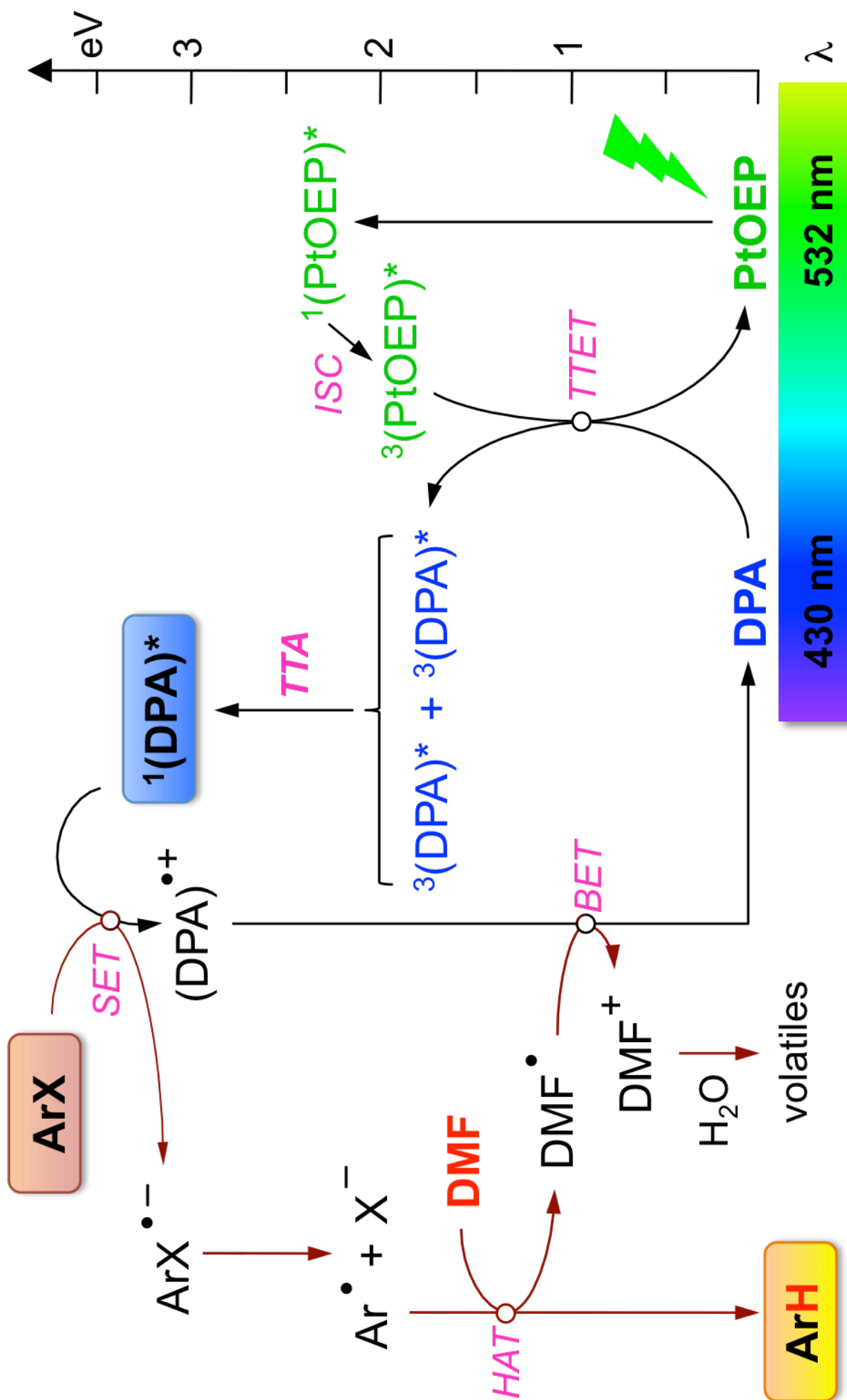


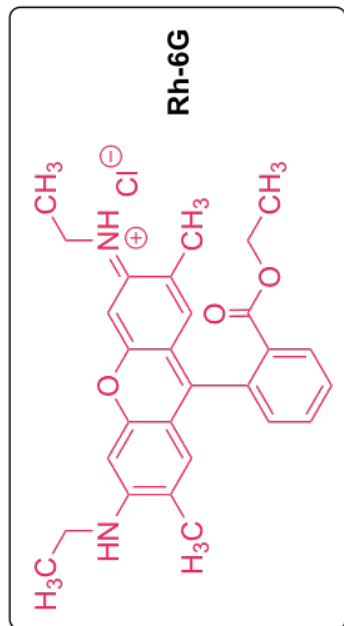
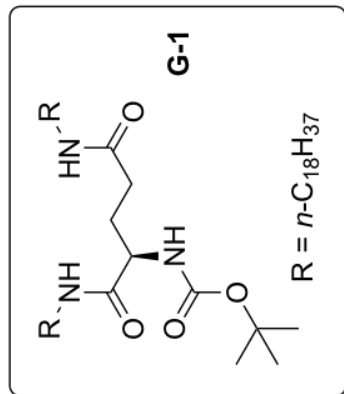






@INTRAGEL in AIR

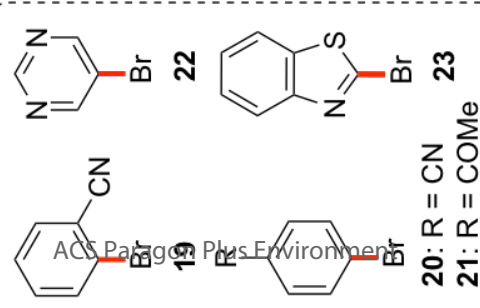




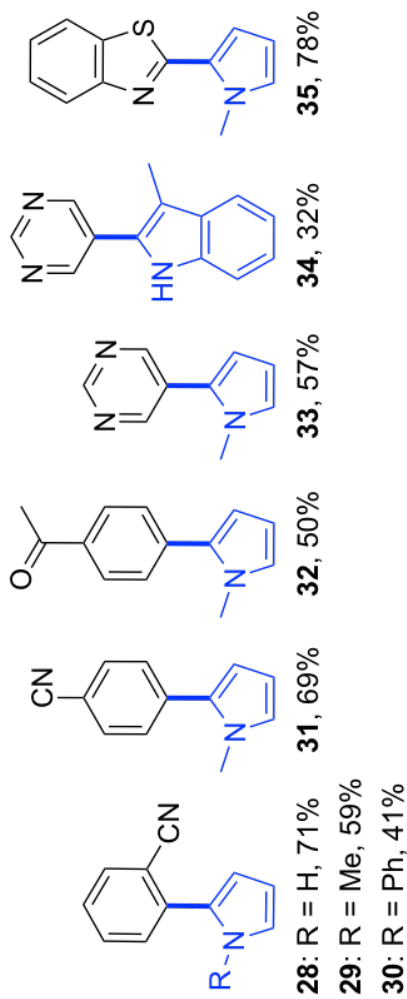
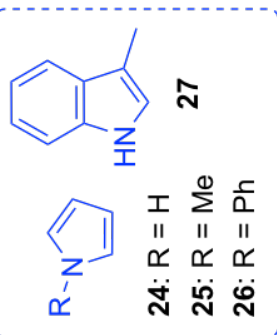
Photoredox catalytic arylations by one-to-one combinations of bromo-compounds and trapping agents

A

Aromatic bromo-compounds



Trapping agents

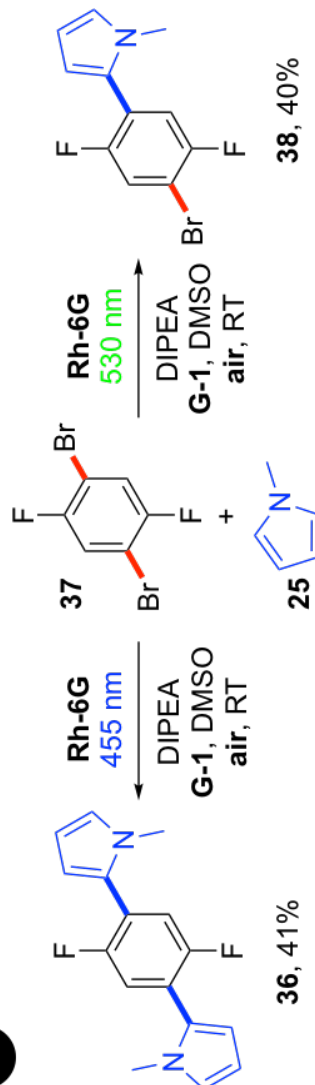


Supramolecular gel
doped with reactants



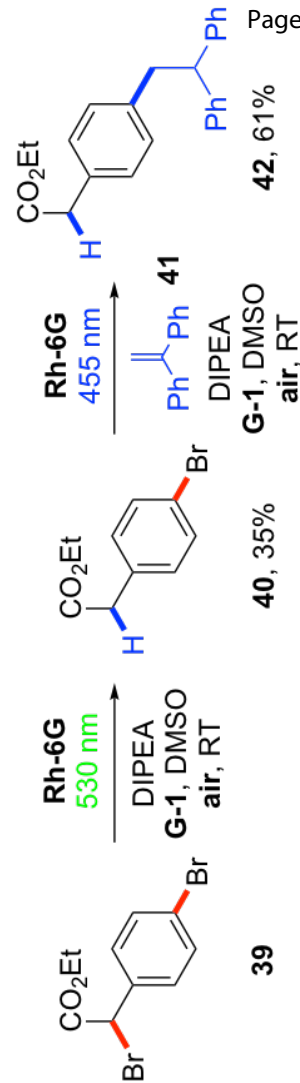
B

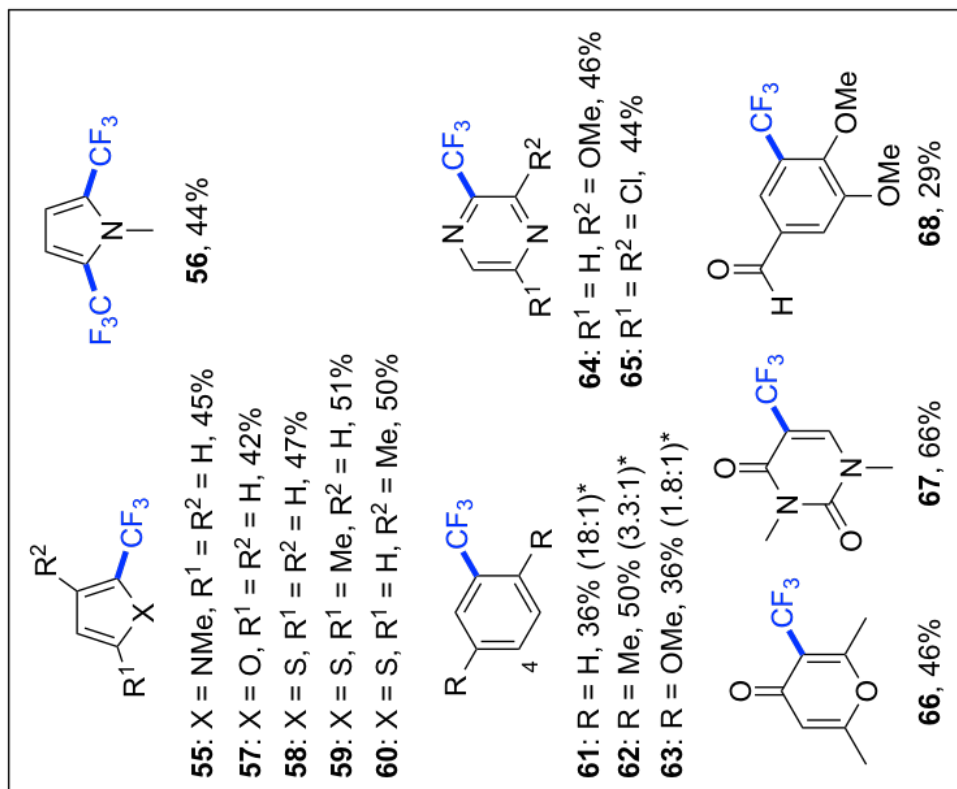
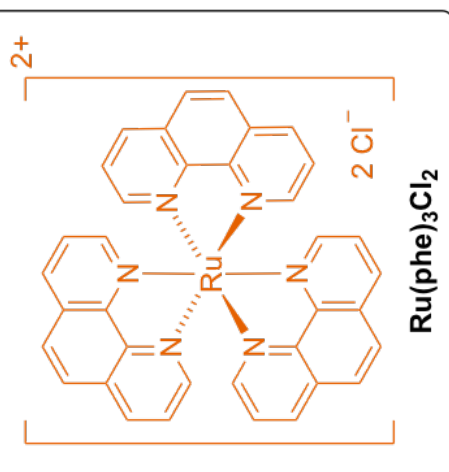
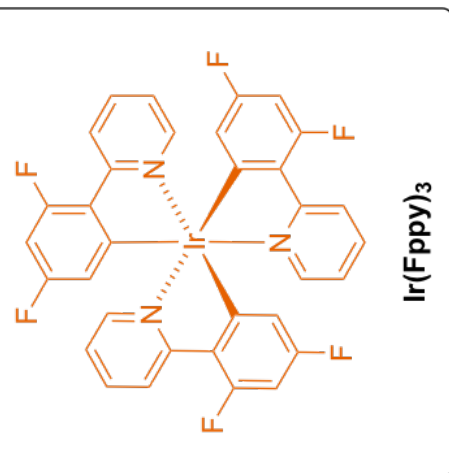
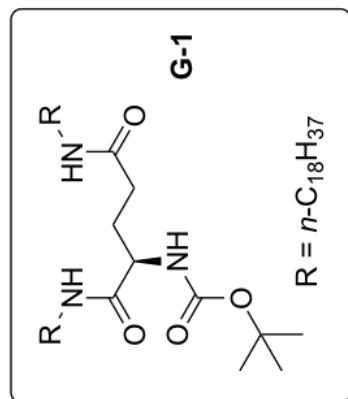
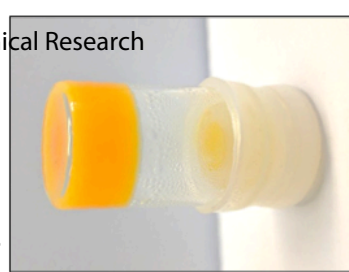
One or two-fold substitutions



C

Sequential substitutions



Supramolecular gel
doped with reactantsRu(phe)₃Cl₂

455 nm

(5-membered rings)

or

Ir(Fppy)₃

365 nm

(6-membered rings)

K₂HPO₄G-1, CH₃CN

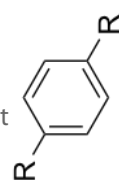
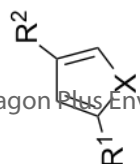
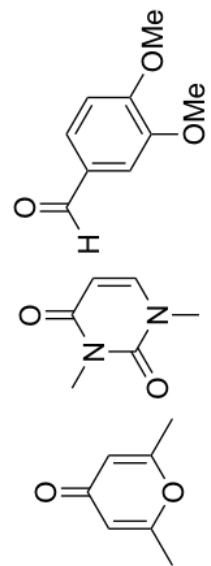
air, RT

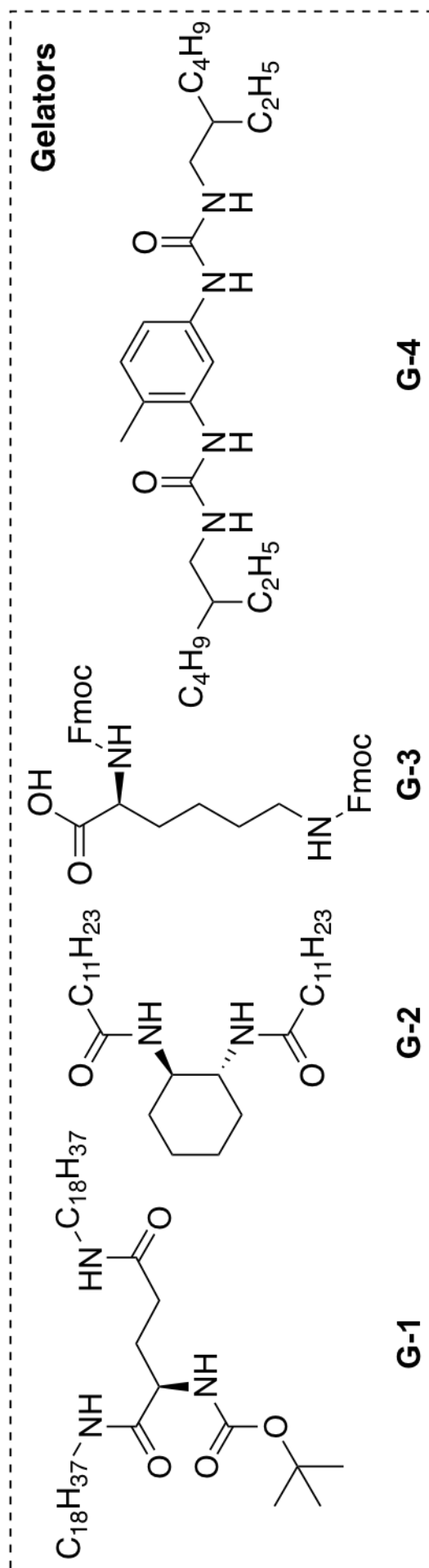
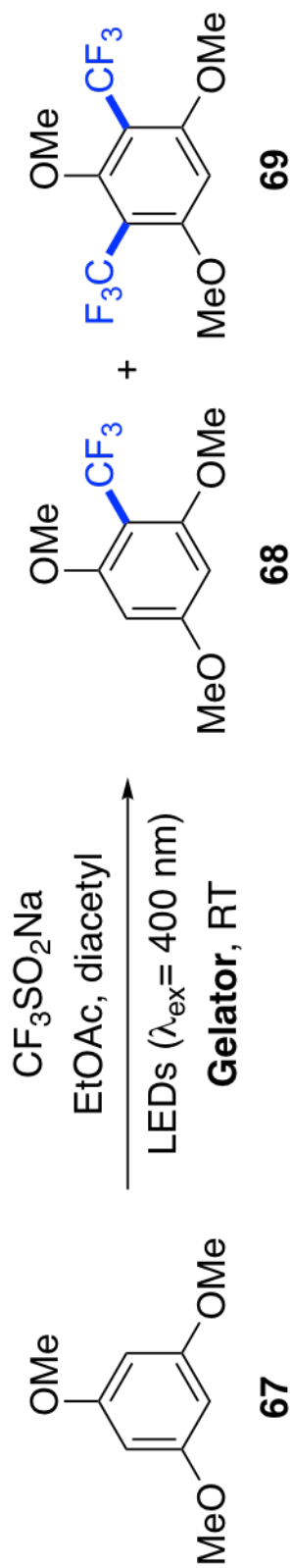
TfCl



+

Arenes and heteroarenes

25: X = NMe, R¹ = R² = H**43:** X = O, R¹ = R² = H**44:** X = S, R¹ = R² = H**45:** X = S, R¹ = Me, R² = H**46:** X = S, R¹ = H, R² = Me**47:** R = H**50:** R¹ = H, R² = OMe**51:** R¹ = R² = Cl**49:** R = OMe**52****53****54**



1
2
3
4
5
6
7
8
9
10
11
12
13
14
15
16
17
18
19
20
21
22
23
24
25
26
27
28
29
30
31
32
33
34
35
36
37
38
39
40
41
42
43
44
45
46
47
48
49
50
51
52
53
54
55
56
57
58
59
60

